# Parity violation in neutron statistical scattering

A. Müller and H. L. Harney
*Max-Planck-Institut für Kernphysik, D-6900 Heidelberg, Federal Republic of Germany*
(Received 4 April 1991)

For nearly 100 nuclei, the rms expectation values of three neutron transmission observables sensitive to parity violation are predicted. Total enhancement factors $\sim 10^2$–$10^4$ in comparison to related observables in nucleon-nucleon scattering are found. To this end, a model of parity violation in the framework of statistical scattering theory is formulated and worked out in detail. General expressions are deduced from it, which connect the expectation values of parity forbidden $S$-matrix elements to average input parameters, namely, level densities, transmission coefficients, and spreading widths. The general results are discussed in terms of the relevant nuclear time scales, and the numerical predictions in terms of a "parity forbidden strength function" and several enhancement factors. Additionally, the role of finite energy resolution, crucial for energy averaging experiments, is studied.

PACS number(s): 11.30.Er, 25.40.Dn, 24.30.Gd, 24.70.+s

## I. INTRODUCTION

Less than ten years after the discovery of parity ($P$) violation in $\beta$ decay, there was a first hint that the order of magnitude of parity forbidden effects in neutron induced reactions is astonishing. The "strength ratio" of the weak to the strong force is of the order of $10^{-7}$, leading to parity forbidden interference effects of the same order of magnitude. But Abov *et al.* [1] found in the reaction $^{113}\mathrm{Cd}(\vec{n},\gamma)^{114}\mathrm{Cd}$ a parity forbidden asymmetry $|\sigma_+-\sigma_-|/(\sigma_++\sigma_-)=(3.7\pm0.9)\times10^{-4}$, where $\sigma_+$ and $\sigma_-$ are the $(n,\gamma)$ cross sections in some direction and its mirror image, respectively. This surprising result was met with doubt by other researchers, but nevertheless led to the first theoretical investigations of possible enhancement mechanisms, also concerning time reversal ($T$) violation [2,3].

We skip the further developments (which can be found in Ref. [4], together with extensive material on experimental results and methods and different theoretical approaches) until 1981, when Alfimenkov *et al.* [5] experimentally confirmed a prediction by Sushkov and Flambaum [6] concerning $P$ violation at the percent level: the helicity dependence of neutron transmission through a $^{139}$La target attained $\sim 10\%$, when the neutron energy was swept through a resonance located at 0.75 eV, and the size of the effect closely followed the resonance line. This effect recently found renewed interest in a quite sophisticated form: in a double target experiment, the parity violating forces were used both to polarize and to analyze an initially unpolarized neutron beam [7]. The findings of Alfimenkov *et al.* prompted a series of theoretical investigations [8–10] going beyond the qualitative prediction of Ref. [6]. The common mechanism invoked in all these papers was the existence of pairs of long-lived, closely spaced *compound* resonances with opposite parity. Their mixing was shown to be enhanced by the smallness of $d$ (level spacing) and the largeness of $1/\Gamma$ (inverse level width) as compared to the mixing of *single* particle resonances. This approach offered quite a detailed understanding, suffering from one drawback only: In order to evaluate the resulting formulae quantitatively, one had to know the parameters of the individual resonances as spin and parity, widths, and spacings. There is no way to calculate the wave functions (and their properties) of resonances in the highly excited ($\sim 8$ MeV) compound nucleus, and the measured data sets are notoriously incomplete, particularly spin/parity assignments and $p$-wave neutron widths.

At this point, a second line of thought enters: the statistical approach to nuclear properties. In 1985, this approach had found a formulation [11] based on a sound theoretical foundation and connecting the statistics of *spectral* properties with those of *scattering* properties, thus largely summarizing prior knowledge. Its final result was an equation for the correlation function of scattering amplitudes for arbitrary numbers and values of transmission coefficients, which, together with the average level densities, were the only necessary input parameters. It was then considered whether or not it is possible to include parity (and other symmetry) violations in the framework of this formalism, and the present work shows how to do so and what results from it. Combining parity violation and the statistical description one gets rid of the *individual* resonance parameters and gains a description of *average* parity violation effects in nuclei.

The purpose of doing so is twofold: First, parity violation in itself is still an interesting subject, especially when it is studied systematically, as it is here in a large number ($\sim 100$) of nuclei. In this sense, the present work for the first time exploits the general predictive power of Ref. [11] in a context of fundamental, not applied science. We feel encouraged about this motivation by a recent measurement [12] of parity violation in $^{238}$U, where effects on the percent level were found and, for the first time, an experimental value of the average perturbation strength was given. Second, studies on enhanced $P$ violation, where much is known, may guide and encourage studies on $T$ violation. Much theoretical work on the latter was already done [13–17] and experimental work is under

 

way [18,19]. It is with this and other possible extensions in mind that we have included extensive lists of input data. For $T$ violation, a systematic quantitative study similar to the present one appears feasible and could make use of the data presented here. In the present work, however, we have restricted ourselves to parity violation and assumed that time reversal invariance holds.

In accordance with these points, the present article is organized as follows: Sec. II gives a phenomenological explanation of parity forbidden observables in neutron optics and of enhancement effects of symmetry violation. Section III contains the precise definition of our model and most of the technical material necessary for its evaluation. The final results are contained in Eqs. (3.12) through (3.24). Section IV is an interpretative discussion of several general features of the model outlined in Sec. III. In Sec. V, the problem of finite energy resolution—a prerequisite for any energy averaging experiment—is treated in some detail. Section VI contains the application to the concrete case of neutron scattering on 99 different nuclei. The general formulas of Sec. III are specialized and numerical results presented, which then are discussed in terms of a rule-of-thumb estimate. The validity of various statements and approximations made in the text is also discussed. The Appendixes A–D contain technical material pertaining to Secs. III–VI, respectively. Appendix D additionally contains tables for the various input data, which are necessary for a check of reliability as well as any further use of the results presented in Sec. VI in different contexts. For a reader mainly interested in the results, Secs. II A, IV A 2, and VI B offer a quick way of reading.

## II. PHENOMENOLOGY: OBSERVABLES AND THEIR ENHANCEMENT

We start by introducing those of the parity forbidden observables which we theoretically investigate in the following sections. A broader range of observables can be found in the literature [4]. Then we give an explanation of the enhancement mechanisms.

### A. Parity forbidden observables in neutron optics

In the present work, we restrict ourselves to the theoretical description of three parity forbidden observables occurring in neutron transmission experiments. They are performed with longitudinally polarized, transversally polarized, and unpolarized neutrons in the entrance channel, respectively, and all are closely analogous to optical phenomena. It should be clear, however, that in the case of neutron scattering, the phenomena are connected with a true parity violation (due to the weak force), whereas in the case of light scattering the left/right discrimination is already built into the spatial shape of the scattering center, i.e., into the chirality of molecules or of crystal structure. The truly $P$-violating nature of the different neutron observables is pointed out by giving the corresponding pseudoscalar quantities.

The first observable is the "helicity dependence of transmitted intensity" and operates with longitudinally polarized neutrons. It is given by

$$A=\frac{N_+-N_-}{N_++N_-}=\frac{N_0e^{-nl\sigma^t_+}-N_0e^{-nl\sigma^t_-}}{N_0e^{-nl\sigma^t_+}+N_0e^{-nl\sigma_-}}\approx-\frac{nl}{2}\Delta\sigma^t$$

$$=-2\pi\frac{nl}{k}\mathrm{Im}(\Delta f(0^\circ))\ , \tag{2.1}$$

where $N^\pm$, $\sigma^\pm$ are the counting rates (in the forward direction) and total cross sections for the two different polarization states (helicities), $\Delta\sigma^t$ is the difference $\sigma^+-\sigma^-$, and $n$ and $l$ are the number density and thickness of the target. The third step in (2.1) is an expansion of $A$ up to first order in $nl\Delta\sigma^t$. The last step follows by virtue of the optical theorem with $\Delta f(0^\circ)=f_+(0^\circ)-f_-(0^\circ)$. The corresponding pseudoscalar is $\mathbf{s}_i\circ\mathbf{k}_i$, where $\mathbf{s}$ and $\mathbf{k}$ are the spin and the wave vector of the neutron and $i$ denotes the entrance channel. The corresponding optical phenomenon is circular dichroism: different values of the absorption coefficient for the two different circular polarization states of light.

The second parity violation observable is "spin rotation" or "neutron optical activity," [20] operating with transversely polarized neutrons and given by

$$\Phi=-kl\ \mathrm{Re}(\Delta n)\approx-2\pi\frac{nl}{k}\mathrm{Re}(\Delta f(0^\circ)) \tag{2.2}$$

(in units of rad), where $k$, $l$, $n$, $\Delta f$ are as before and $\Delta n=n_+-n_-$ is the difference of the indices of refraction for the two different helicities. The second [20] equation comes from the neutron optical relation between index of refraction and scattering amplitude [21]. The transverse polarization in the entrance channel is a *coherent* mixture of the two longitudinal polarizations (helicities); if the index of refraction and thus the wave vector inside the target is different for the two different polarizations, there will be a phase shift leading to a rotation of the transverse polarization. The effect can be understood in terms of a parity violating force proportional to $\mathbf{s}_i\circ\mathbf{k}_i$ and the optical analogy is optical activity: two different values of the index of refraction for the two different circular polarization states of light.

The last parity violation observable in our context is "polarization of the emitted particle," [20] operating with unpolarized neutrons in the entrance channel and given by

$$P=\frac{N_+-N_-}{N_++N_-}\approx-2\pi\frac{nl}{k}\mathrm{Im}(\Delta f(0^\circ))\ , \tag{2.3}$$

where $N_\pm$ are the counting rates for neutrons with different helicities in the exit channel and the related pseudoscalar is $\mathbf{s}_f\circ\mathbf{k}_f$. In distinction to $\Phi$, we are dealing here with an *incoherent* mixture of polarizations with equal weights in the entrance channel. Again, if the interaction is different for the two helicities, they will be scattered out of the beam differently, leading to an unbalanced mixture and thus to a net polarization in the exit channel. The two quantities $P$ and $A$ are numerically identical and their main difference is that for $A$ the ex-

perimental setup is that of an analyzer, and for $P$ that of a polarizer.

The raw effects are thus all expected to rise linearly with the target thickness [cf. Eqs. (2.1)–(2.3)]; on the other hand, the statistical error increases with decreasing counting rate. Hence, there is an optimum target thickness,

$$l_{\text{opt}}=2l_0=2/n\sigma^t\ , \tag{2.4}$$

where $l_0$ is the mean free path. This results in

$$A_{\text{opt}}=P_{\text{opt}}=-4\pi\frac{1}{\sigma^t k}\text{Im}(\Delta f(0^\circ))\ ,$$
$$\Phi_{\text{opt}}=-4\pi\frac{1}{\sigma^t k}\text{Re}(\Delta f(0^\circ))\ . \tag{2.5}$$

It now clearly appears that all parity violation observables in neutron transmission are closely related to one and the same difference of scattering amplitudes. The calculation of this difference in the framework of statistical scattering theory is the subject of the following chapter. Before that, we briefly turn to the very reason motivating the whole work.

### B. Explanation of enhancement mechanisms

The discovery and description of these mechanisms already dates back more than 20 years to early work of Ericson [2] and Shapiro [3], where clear explanations for all but one of them can be found. Shapiro also introduced the relative measure of interaction strength of the weak perturbation $H^w$ to the unperturbed Hamiltonian $H^0$, which is at the same time the order of magnitude of the parity violating scattering amplitude on the level of the nucleon-*nucleon* interaction:

$$F^w_{NN}\approx\left[\frac{\text{Tr}[(H^w)^2]}{\text{Tr}[(H^0)^2]}\right]^{1/2}\approx 1.50\times10^{-7}\ . \tag{2.6}$$

This order of magnitude is well established [22–24] and the precise value we have taken is from proton-proton-scattering experiments [23]. Physically such an ansatz measures the strength of an interaction (with respect to another one) in the sense of an rms element, because for an operator $H$ with dimension $\Lambda$ we have

$$\frac{(\text{Tr}[H^2])^{1/2}}{\text{Dim}[H]}=\frac{1}{\Lambda}\left[\sum_{\mu\nu}H^2_{\mu\nu}\right]^{1/2}\ . \tag{2.7}$$

Also mathematically (2.6) is an expression for the "strength" of an interaction operator, because $(\text{Tr}[H^2])^{1/2}$ is a matrix norm (the so-called Frobenius norm, a special case of the Hölder norm [25]).

All enhancement effects express themselves in the occurrence of parity violating amplitudes in nucleon-*nucleus* scattering, which can be much larger than (2.6). Possible mechanisms are as follows.

*Kinematic and structural enhancement.* Consider the scattering scheme in Fig. 1: an incoming scattering wave $|i_\pi\rangle$ with parity $\pi$ couples to a metastable resonance $|\rho_\pi\rangle$ with the same parity, which, in turn, decays back with amplitude $Z_+$ to a final scattering state $|f_\pi\rangle$ with still

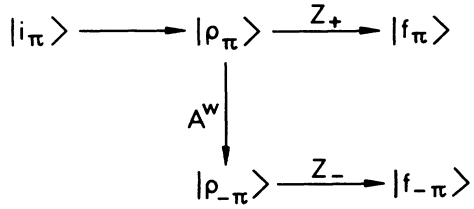


FIG. 1. Scattering scheme with a parity forbidden transition. The meaning of the symbols is as follows: $|i\rangle$ ($|f\rangle$), initial (final) channel; $\pi$, parity, $|\rho\rangle$, scattering resonance; $A^w$,$Z$, transition and decay amplitudes. See Sec. II B for further explanation.

the same parity. If there is parity violation, there is a second branch in the reaction scheme: a parity violating coupling $A^w$ of the first resonance to a second one $|\rho_{-\pi}\rangle$ with opposite parity; the latter one then decays with the amplitude $Z_-$ to a final scattering state $|f_{-\pi}\rangle$ with parity $-\pi$. ($|f_\pi\rangle$ and $|f_{-\pi}\rangle$ can be, e.g., electric and magnetic multipole radiation of the same multipolarity $l$.) This leads to the following final state:

$$|f\rangle\approx\frac{Z_+|f_\pi\rangle+A^wZ_-|f_{-\pi}\rangle}{\sqrt{|Z_+|^2+|A^wZ_-|^2}}$$
$$\approx\exp(i\arg Z_+)\left[|f_\pi\rangle+A^w\frac{Z_-}{|Z_+|}|f_{-\pi}\rangle\right]\ , \tag{2.8}$$

where we have assumed $|A^w|\ll1$. Now, the ratio of $Z_-/|Z_+|$ can, under certain circumstances, be much larger than 1. This is for reasons both of specific nuclear structure (Shapiro [3] discusses the example of a pair of $\gamma$ channels as mentioned above) and of kinematics (playing an important role in the neutron scattering experiments we have in mind here). Note the difference between $A^w$ and $F^w_{NN}$ introduced in Eq. (2.6): $A^w$ is a *transition* amplitude between resonance states, $F^w_{NN}$ is a *scattering* amplitude between continuum states. Their connection will become clearer below.

*Dynamic enhancement.* In perturbation theory—certainly applicable to the weak interaction—the transition amplitude is proportional to the ratio of perturbation ($w$) to level distance ($d$), i.e.,

$$A^w\propto\frac{w}{d}\ . \tag{2.9}$$

Here, $w$ shall be a typical matrix element of $H^w$. In (2.9) it is not divided by a typical strong matrix element [as in (2.6)] but by the level distance. For highly excited and heavy nuclei, $d$ can be very small, down to fractions of an eV. Thus we see that already the weak transition amplitude $A^w$ inside the compound nucleus is an "enhanced" quantity.

*Resonance enhancement.* Consider the transition between two resonance states $|\rho_+\rangle$ and $|\rho_-\rangle$ with different parities. It is described by the evolution operator $\exp(-iHt/\hbar)$ with $H=H^0+H^w$, where $H^w$ connects $|\rho_+\rangle$ and $|\rho_-\rangle$. Let the resonances have (for the sake of

simplicity) equal widths $\Gamma$, corresponding to a lifetime $\hbar/\Gamma$. Introducing the latter one for $t$ and expanding to lowest order in $H^w/\Gamma$ one gets for the transition amplitude:

$$A^w \propto \langle \rho_- | e^{-i(H^0+H^w)/\Gamma} | \rho_+ \rangle \approx \frac{w}{\Gamma} \ . \tag{2.10}$$

It is thus clear that narrow resonances with long lifetimes enhance the effect, motivating the notion of "lifetime enhancement": we have two channels with a small "cross talk." The longer this cross talk holds on, the more signal will be accumulated in the "wrong" channel.

After this qualitative reasoning, we now turn to a quantitative model.

## III. FORMALITIES: MODEL AND RESULTS

### A. From the scattering amplitude to the Hamiltonian

Here, there are three steps: first, the helicity-dependent difference of the forward scattering amplitude is given in terms of the scattering matrix; second, the scattering matrix is expressed in terms of the Hamiltonian; last, the Hamiltonian with its statistical and parity violating features is given.

#### *1. Connection observables—scattering matrix*

The relevant helicity dependent difference of the forward scattering amplitudes for a spin-$\frac{1}{2}$ projectile, impinging on a target with spin $I$ is given by

$$\Delta f(0°) = f_+(0°) - f_-(0°)$$
$$= \frac{2i}{k} \sum_{\substack{l=1 \\ J}} \Delta_{I,j=l-\frac{1}{2},J} \frac{2J+1}{2(2I+1)} S^{j=l-\frac{1}{2},J}_{l,l-1} \ , \tag{3.1}$$

where we have used the coupling scheme $j = l + \frac{1}{2}$, $J = j + I$ and where $\Delta_{I,j,J}$ stands for the selection (triangle) rule $|I-j| \le J \le I+j$; i.e., it is 1 for the selection rule fulfilled, 0 otherwise. [The calculations leading to (3.1) are lengthy and involve cumbersome notations, but they are conceptually uninteresting and thus omitted. For a check we mention that (3.1) coincides with a result published elsewhere in the literature [26].] The dynamics resides in the neutron elastic scattering matrix element $S^{j,J}_{l,l'}$, where from the complete channel index $c$ only $l,j,J$ have been retained: $j$, $J$ as superscripts, indicating that we have to take diagonal elements of $S$ in these labels (as in the omitted labels as well); and $l,l' = l-1$ as subscripts, indicating that parity violation is connected with a change of angular momentum: the parity forbidden $S$-matrix element connects partial waves, which differ by just one unit of $l$ and thus have different parities $\pi = (-1)^l$. In the following, from the complete channel parity $\pi_c = \pi_{\text{proj}} \pi_{\text{targ}} \pi_l$ only the parity factor of the partial wave is retained.

For nucleons up to 10 keV the centrifugal barrier factor is $kR \ll 1$ and thus the restriction to $s$ and $p$ waves fully justified ("$p$-wave approximation"), leading to the following simple expression:

$$\Delta f(0°) = \frac{2i}{k} \left[ \frac{I+1}{2I+1} S^{\frac{1}{2},I+\frac{1}{2}}_{1,0} + \frac{I}{2I+1} S^{\frac{1}{2},I-\frac{1}{2}}_{1,0} \right] , \quad kR \ll 1 \ . \tag{3.2}$$

Still simpler is the expression for target spin $I = 0$:

$$\Delta f(0°) = \frac{2i}{k} S^{\frac{1}{2},\frac{1}{2}}_{1,0} \ . \tag{3.3}$$

We now turn to the construction of the $S$ matrix in terms of the Hamiltonian.

#### *2. Connection scattering matrix—Hamiltonian*

We start out from the equations [27]

$$S^{CN}_{ab} = \delta_{ab} - 2\pi i V^T_{a\mu} G_{\mu\nu} V_{\nu b} \ , \tag{3.4}$$

where $a,b = 1, \ldots, N$ and $\mu,\nu = 1, \ldots, \Lambda$,

$$G = (E - H + i\pi V V^T)^{-1} \ , \tag{3.5}$$

where the orthogonality relation

$$\sum_\mu V_{\mu a} V_{\mu b} = \mathbf{V}_a \circ \mathbf{V}_b = \Lambda v_a^2 \delta_{ab} \tag{3.6}$$

shall hold. Here, $V$ is a rectangular matrix describing the coupling of $\Lambda$ metastable compound nucleus states or bound states embedded in the continuum (greek subscripts) to $N$ scattering channels (latin subscripts), its columns $\mathbf{V}_c = (V_{1c}, \ldots, V_{\Lambda c})^T$ are the "coupling vectors" to a specific channel, $\Lambda v_c^2$ are their norms, and $G$ is the Green function or "propagator" in the subspace of the compound states.

There are some approximations inherent in the form (3.4)–(3.6): First, we have neglected direct interactions, which is entirely justified for slow neutrons ("slow neutron approximation"); formally, this leads to Eq. (3.6). Note that this relation is, in its essence, a statistical one: if the coupling vectors $\mathbf{V}_c$ are mutually uncorrelated, the sum in (3.6) runs for $a \neq b$ over random-sign terms, and we have $\Lambda^{-1} \mathbf{V}_a \circ \mathbf{V}_b \sim v_a v_b / \sqrt{\Lambda}$, whereas $\Lambda^{-1} |\mathbf{V}_a|^2$ is independent of $\Lambda$. Taking the limit $\Lambda \to \infty$, we are led to (3.6). Second, no energy dependence of the coupling $V$ whatsoever has been assumed, which, in particular, precludes threshold effects. Thus, the forthcoming results are numerically reliable only in some distance to the neutron threshold. Third, we should have included the potential scattering phase shifts; but they drop out of our final results and so we omitted them from the outset.

Four important properties of the $S$ matrix or Green function shall be noted in connection with Eqs. (3.4) and (3.5). First, causality: formally this is ensured by the fact that all poles are lying in the lower half of the complex plane. Second, unitarity: formally, this can be seen from the form of the so-called Ward identity [11]

$$G V V^T G^* = -\frac{1}{\pi} \mathrm{Im}(G) \ , \tag{3.7}$$

where unitarity in the common form $SS^\dagger = \mathbf{1}$ follows by combining it with (3.4). Third, we have the analytic property

$$G^2=-\frac{\partial}{\partial E}G\ , \tag{3.8}$$

analogously for higher powers and $G^*$. Fourth, symmetry: $S=S^T$ holds, if we take $H$ and $V$ to be real; this is ensured by time reversal invariance, which we will assume throughout the present work.

Together with the expressions in Sec. II we now are at the end of the sequence "observables → scattering amplitude → scattering matrix → Hamiltonian." Next we turn to the formulation of both the statistical nature and parity violation of compound nucleus scattering on the level of the underlying Hamiltonian.

### B. Statistics and parity violation in the compound nucleus interaction

To describe parity violation, the Hamiltonian occurring in Eq. (3.5) is assumed to have the following form:

$$H=H^0+H^w=\begin{bmatrix} H^+ & \emptyset \\ \emptyset & H^- \end{bmatrix}+\begin{bmatrix} H^{++} & H^{+-} \\ H^{-+} & H^{--} \end{bmatrix}\ . \tag{3.9}$$

The blocks $H^+$, $H^-$ are restricted to the subspaces of given parity and thus describe the parity allowed interaction within such a subspace, whereas $H^w$ connects all states with each other, the blocks $H^{+-}$, $H^{-+}$ describing the parity forbidden interaction between subspaces of different parity. Both $H^0$ and $H^w$ respect rotational symmetry and thus connect resonances of the same total angular momentum $J$.

In order to model the "unpredictable" and "uncalculable" residual interaction in the highly excited compound nucleus, both $H^0$ and $H^w$ shall belong to a Gaussian orthogonal ensemble (GOE), i.e., their matrix elements are uncorrelated Gaussian variables with their variances given as follows:

$$\overline{H^{\pm}_{\mu\nu}H^{\pm}_{\mu'\nu'}}=\frac{\Lambda^{\pm}}{\pi^2}(d^{\pm})^2(\delta_{\mu\mu'}\delta_{\nu\nu'}+\delta_{\mu\nu'}\delta_{\nu\mu'})\ , \tag{3.10}$$

$$\overline{H^w_{\mu\nu}H^w_{\mu'\nu'}}=w^2(\delta_{\mu\mu'}\delta_{\nu\nu'}+\delta_{\mu\nu'}\delta_{\nu\mu'})\ . \tag{3.11}$$

Here, $\Lambda^{\pm}$ and $d^{\pm}$ are the numbers and average level distances of the compound states with a given parity, and $w^2$ is the strength parameter of the weak interaction. (With $H^{\pm}$ and $H^w$ acting within a subspace of given $J$ they had to carry, in principle, an additional superscript $J$, as well as all related quantities, e.g., $d^{J\pm}$ and so on. The following considerations holding for fixed $J$, we drop this superscript for notational convenience. In Sec. VI, when we have to discriminate between different $J$, we shall resume the extended notation.) The somehow artificial way of defining the variances of $H^{\pm}$ is for the mere sake of convenience: we want to be in accordance with the article of Verbaarschot *et al.* [11], which is fundamental for the present work. In Ref. [11] also a more extensive motivation for the use of random Hamiltonians may be found, as well as an introduction to the mathematical techniques. An important point of the whole ansatz is an ergodic hypothesis: averages over quantities (cross sections, correlations, and so on) fluctuating with *energy* are replaced by averages over the *ensemble* of random Hamiltonians. We now restrict ourselves to cite a series of successful applications of the GOE [28–30], especially to other questions of symmetry violation [31,16,17] and to give the result for the parity forbidden scattering matrix element in the language of Verbaarschot *et al.* [11] (in the following, $p$ and $m$ stand for two channels with opposite parity):

$$\overline{S}=\overline{S^0}\ , \tag{3.12}$$

$$\overline{S^{PV}_{pm}}=0\ , \tag{3.13}$$

$$\overline{S^{PV}_{pm}(S^{PV}_{p'm'})^*}=\left[\frac{w}{\hbar}\right]^2\overline{Q_{pp}}\ \overline{Q_{mm}}\,\delta_{pp'}\delta_{mm'}\ , \tag{3.14}$$

$$\overline{Q_{pp}}=2\pi\hbar\overline{[(V^+)^TG^+(G^+)^*V^+]_{pp}}\ , \tag{3.15}$$

where $S^0$ is the unperturbed scattering matrix obtained by setting $H=H^0$ in Eq. (3.5), $G^+$ and $V^+$ are as in Eqs. (3.5) and (3.6), specialized to the positive parity subspace, and $\overline{Q_{pp}}$ [or $\overline{Q_{mm}}$ with the replacement $+\rightarrow-$ in Eq. (3.15)] stands for a threefold integration of the type of equation (8.13) of Verbaarschot *et al.* [11], which will be explicitly given below. Before that, some comments on Eqs. (3.12)–(3.15): (i) All of them are true up to second order in the perturbation $H^w$ ("weak interaction approximation") and to zeroth order in $\Lambda^{-1}$ ("many resonance approximation," which has already been used in the underlying work [11]). (ii) The average $S$ matrix remains unchanged [Eq. (3.12)]; this is important for the transmission coefficients $T_c$, which are closely connected to $\overline{S}_{cc}$. (iii) In particular, there is no parity violation on average [Eq. (3.13)]. This is reasonable, because, at a given energy, the parity forbidden effect is due to interference of the strong and of the weak interaction; if the energy is changed, the phase of the compound nucleus states and thus the sign of the interference effect should fluctuate in a random manner, leading to a vanishing average value. If this argument became questionable by recent experimental findings (see Sec. VII), our model still remains valid for the fluctuating part of $S^{PV}$ alone. (iv) Due to similar arguments, scattering matrix elements for different pairs of entrance and exit channels are uncorrelated.

For the observables of Sec. II one has to know either the real or the imaginary part of $\Delta f$ as it is given by Eq. (3.1). In the framework of the statistical model developed here, we now ask for averages and variances of $\mathrm{Im}(\Delta f)$ and $\mathrm{Re}(\Delta f)$. It is not difficult to show that no other quantities are needed than those already given in Eqs. (3.12)–(3.15):

$$\overline{\mathrm{Im}(\Delta f)}=\overline{\mathrm{Re}(\Delta f)}=\overline{\Delta f}=0\ , \tag{3.16}$$

$$\overline{\mathrm{Im}^2(\Delta f)}=\overline{\mathrm{Re}^2(\Delta f)}=\tfrac{1}{2}\overline{|\Delta f|^2}$$
$$=\frac{2}{k^2}\sum_{l=1}^{J}\Delta_{I,l-\frac{1}{2},J}\left[\frac{2J+1}{2(2I+1)}\right]^2\overline{|S^{j=l-\frac{1}{2},J}_{l,l-1}|^2}\ . \tag{3.17}$$

We finish this section by giving the explicit form of the two-point functions $Q$ occurring in (3.14) and (3.15)

(given for channel $p,m$ is analogous; for a derivation see Appendix B):

$$\overline{Q_{pp}}=\frac{1}{8}\int_0^\infty d\lambda_1\int_0^\infty d\lambda_2\int_0^1 d\lambda\,\mu(\mathbf{\Lambda})\prod_{\vec{T}}(\mathbf{\Lambda})q_p(\mathbf{\Lambda})\ , \tag{3.18}$$

where $\mathbf{\Lambda}$ is the vector $(\lambda_1,\lambda_2,\lambda)$, $\mu$ is the "measure" function

$$\mu(\mathbf{\Lambda})=\frac{(1-\lambda)\lambda|\lambda_1-\lambda_2|}{\sqrt{(1+\lambda_1)(1+\lambda_2)}\sqrt{\lambda_1\lambda_2}(\lambda_1+\lambda)^2(\lambda_2+\lambda)^2}\ , \tag{3.19}$$

and $\prod$ the product function of Verbaarschot *et al.*:

$$\prod_{\vec{T}}(\mathbf{\Lambda})=\prod_{p'=1}^{N}\frac{1-T_{p'}\lambda}{\sqrt{1+T_{p'}\lambda_1}\sqrt{1+T_{p'}\lambda_2}}\ , \tag{3.20}$$

with $p'$ running over all channels with the same $J^\pi$ as the channel $p$. The transmission coefficient $T_c$ of channel $c$ is connected with the coupling $V$ as follows:

$$T_c=\frac{4x_c}{(1+x_c)^2} \tag{3.21}$$

with

$$x_c=\pi^2\frac{\frac{1}{\Lambda}\sum_\lambda V_{\lambda c}^2}{d}\ . \tag{3.22}$$

Note that the numerator in (3.22) is the arithmetic average of the squared coupling elements $V_{\lambda c}$.

The remaining part of the integrand is specific for the problem under consideration:

$$q_p(\mathbf{\Lambda})=2\pi\frac{\hbar}{d^+}T_p\left[\frac{\lambda_1(1+\lambda_1)}{1+T_p\lambda_1}+\frac{\lambda_2(1+\lambda_2)}{1+T_p\lambda_2}+\frac{2\lambda(1-\lambda)}{1-T_p\lambda}\right]\ . \tag{3.23}$$

For later use we introduce a dimensionless quantity related to $Q$:

$$\bar{L}_p=\frac{\overline{Q_{pp}}}{h/d^+}\ , \tag{3.24}$$

where $h$ is Planck's constant. Equations (3.12) through (3.24) are the *formal* result of this work. We now come to some simplifications.

### C. Some useful approximations

The first approximation is connected with the fact that compound nucleus resonances are often coupled to a large number of open channels; here the word "channel" has to be understood in the strict sense of labeling precisely *one* scattering state, i.e., giving *all* its quantum numbers including fragmentation and possible internal excitation of the fragments. This especially holds for the multitude of $\gamma$ channels, corresponding to the different $\gamma$ energies and excitations of the residual nucleus. It is impossible to know all the individual transmission coefficients of these channels. But there is a way out of this problem: let $l=1,\ldots,N_l$ be a subset of channels with the property

$$\frac{T_l}{\sum_{l'=1}^{N_l}T_{l'}}\sim N_l^{-1}\ll 1\quad\text{for } l,l'=1,\ldots,N_l\ . \tag{3.25}$$

Then it can be shown that to a very good accuracy (see Appendix A) the following "lumping" approximation holds:

$$\prod_l^{N_l}\frac{1-T_l\lambda}{\sqrt{1+T_l\lambda_1}\sqrt{1+T_l\lambda_2}}\approx e^{-(\lambda_1+\lambda_2+2\lambda)T_L/2}\ , \tag{3.26}$$

i.e. the product function of Eq. (3.20) containing many $T_l$ can be replaced by an exponential containing only their sum $T_L$.

The second approximation is connected with the fact that later on we shall apply our results to slow neutron transmission experiments. Physically, this is the case of isolated resonances or "weak absorption" with

$$\sum_c^N T_c\ll 1\ . \tag{3.27}$$

This assumption makes it possible to reduce the triple integration of the type (3.18) to a single one in a quite general class of two-point [32–34] and four-point functions [35]. The result for our special two-point function here is merely stated, its derivation very closely following the mathematical way of reasoning of Ref. [33]:

$$\overline{L_p}\approx\frac{T_p}{2}\int_0^\infty dx\,(1+T_px)^{-1}\prod_{p'}(1+T_{p'}x)^{-1/2}\ , \tag{3.28}$$

with $p'$ running over channels with the same $J^\pi$ as the channel $p$. By numerical evaluation of the full threefold integration (3.18), as described by Verbaarschot [28], approximation (3.28) was shown to be very good.

The third approximation is a combination of the first two, and we shall present it in two different forms: (i) Assuming the lumping approximation for all channels *but* the entrance channel, i.e., $T_L^+=\sum_{p'\neq p}T_{p'}$, we obtain

$$\overline{L_p}\approx 1-xe^{x^2/2}\int_x^\infty dy\,e^{-y^2/2},\quad x=\sqrt{T_L^+/T_p}\ . \tag{3.29}$$

(This integral can be found in the literature [36] as Dawson's integral.) (ii) Assuming the lumping approximation for *all* channels we have to include the factor $(1+T_px)^{-1}$ of Eq. (3.28) in the lumped product function

$$T_L^+=\sum_{p'}T_{p'}+2T_p \tag{3.30}$$

and consequently

$$\overline{L_p}=\frac{T_p}{T_L^+}=\frac{T_p}{3T_p+\sum_{p'\neq p}T_{p'}}\sim\frac{T_p}{\sum_{p'}T_{p'}}\ , \tag{3.31}$$

i.e., essentially the branching ratio of the entrance chan-

nel. The second version in (3.31) exhibits an interesting feature: the factor 3 multiplying the transmission coefficient of the elastic channel ($p$ = entrance = exit channel) is connected in statistical scattering theory to a quantity known as "elastic enhancement factor," which has been thoroughly studied for nuclear [28,37] and light [38] scattering.

The last form of (3.31) results from applying $T_p \ll \sum T_{p'}$ once more.

## IV. INTERPRETATION

In the developments so far there are some assumptions as well as results which deserve further explanation and interpretation. We start with the following.

### A. Form and scaling of the perturbation

#### 1. Nonstatistical perturbation

Our ansatz has been a statistical one not only for the unperturbed Hamiltonian $H^0$, but also for the parity violating perturbation $H^w$, cf. Eqs. (3.10) and (3.11). This latter assumption can be dropped and $H^w$ taken as a much more general matrix with nearly arbitrary fixed elements. This seems astonishing, because how then shall the multitude of independent matrix elements $H^w_{\mu\nu}$ be condensed in the single parameter $w^2$, which is the variance of the Gaussian ansatz according to (3.11)?

The argument is as follows: $H^w$ has to be introduced into Eq. (3.5), the Green function has to be expanded up to second order in $H^w$, and then the average has to be carried out, but now over $H^+$, $H^-$ alone. This leads to the treatment of two-point functions of the form $G_{\mu\nu}G^*_{\mu'\nu'}$ and a following contraction of the indices with $H^w$ and $V$. The result of this contraction is (in leading order of $1/\Lambda$)

$$\bar{S} = \overline{S^0} , \tag{4.1}$$

$$\overline{|S^{PV}_{pm}|^2} = \left[ \frac{1}{\Lambda_+ \Lambda_-} \frac{\mathrm{Tr}[H^{+-}(H^{+-})^T]}{\hbar^2} \right] \overline{Q_{pp}}\,\overline{Q_{mm}} . \tag{4.2}$$

Here, only one additional assumption entered, namely, that the rows of the perturbation operator $H^w$ are not correlated with the coupling vectors, i.e. that the following estimate holds:

$$\frac{[(V^+)^T H^{+-} V^-]_{pm}}{\mathrm{Tr}[H^{+-}(H^{+-})^T]} \sim \frac{[(V^-)^T H^{-+} V^+]_{mp}}{\mathrm{Tr}[H^{+-}(H^{+-})^T]} \sim \frac{1}{\Lambda} . \tag{4.3}$$

This is essentially the random interference argument already used in Sec. III A 2.

Henceforth, only an orthogonally invariant trace is left from the nonstatistical $H^w$, which allows a "gauging" of the variance $w^2$ of the statistical one:

$$w^2 = \frac{1}{\Lambda_+ \Lambda_-} \mathrm{Tr}[H^{+-}(H^{+-})^T] . \tag{4.4}$$

Here, a formally quite satisfying feature is clearly brought up: the orthogonal invariant serving as a gauge of $w^2$ and hence of the "strength" of the perturbation is precisely the matrix norm introduced in Eq. (2.6) (or its generalization to rectangular matrices).

*Interpretation.* An arbitrary fixed perturbation cannot be distinguished from a Gaussian one. The dominant interaction (the two GOE's $H^+$ and $H^-$) alone provides sufficient fluctuations to average out a single orthogonal invariant from a multitude of perturbation elements: the arithmetic mean of the squared matrix elements.

#### 2. Introduction of the spreading width

The next question is: What ansatz has to be chosen for the perturbation parameter $w^2$? The answer to this question is guided by the investigations of other symmetry violations (isospin [31] and time reversal [39]) and has two parts: First, not $w$, but rather the quantity

$$\Gamma^{\downarrow}_w = 2\pi \frac{w^2}{d} \quad (d = \sqrt{d^+ d^-}) , \tag{4.5}$$

the weak "spreading width," is widely independent of the excitation energy and target nucleus and can be considered, in some sense, as the universal parameter of parity violation in nuclear matter. An intuitive explanation of the mere fact of relative constancy can be found in several articles [2,3,40]. We take $\Gamma^{\downarrow}_w = 1.0 \times 10^{-7}$ eV, a value recently measured [12] in neutron scattering on $^{238}$U.

Second, the order of magnitude of $\Gamma^{\downarrow}_w$ is connected with the strength of parity violation in the nucleon-nucleon-interaction [see Eq. (2.6)]:

$$\Gamma^{\downarrow}_w / \Gamma^{\downarrow}_s = \overline{(H^w_{\mu\nu})^2} / \overline{(H^0_{\mu\nu})^2} \approx (F^w_{NN})^2 \approx 2.3 \times 10^{-14} . \tag{4.6}$$

Our choice for $\Gamma^{\downarrow}_w$ and $F^w_{NN}$ implies $\Gamma^{\downarrow}_s \approx 4.3$ MeV. This value satisfactorily compares with the value found from the study of isospin breaking in compound nucleus reactions: Here, the Coulomb spreading width is roughly $\Gamma^{\downarrow}_C \approx 30$ keV and the strength parameter is the electromagnetic fine-structure constant, $(F^C_{NN})^2 \approx \frac{1}{137}$; consequently, from isospin breaking one estimates $\Gamma^{\downarrow}_s \approx 4.1$ MeV. It should be kept in mind, however, that the constancy of spreading widths and thus of ratios like (4.6) holds, in general, only approximately [31,41]. Note that the ansatz (4.6) is based on a specific many particle structure: the strong spreading width $\Gamma^{\downarrow}_s$ being given by the residual interaction of the strong force, which, in turn, is of two-body nature, (4.6) means assuming a weak interaction of two-body nature, too. Otherwise, the spreading width ratio (4.6) could not be independent of the particle number $A$. It is interesting that one-body forces, i.e., a parity violating potential, lead upon averaging to much smaller typical effects [42] than we have found, namely, $10^{-6}$ instead of $10^{-3}$ (see Sec. VI). Note, however, that we are going to calculate *root-mean-square* averages of parity forbidden observables (given by $\overline{|S^{PV}|^2}^{1/2}$), whereas the authors of Ref. [42] calculated averages as such (given by $\overline{S^{PV}}$), which vanish in our model [see Eq. (3.13)] due to random interference.

In this context, the following consideration is enlightening: As can be seen from (3.14) and (3.24), the "parity

forbidden cross section" $\overline{|S^{PV}|^2}$ contains a prefactor

$$\left[2\pi\frac{w}{d}\right]^2=2\pi\frac{\Gamma_w^{\downarrow}}{d}=2\pi\frac{\Gamma_w^{\downarrow}}{\Gamma_s^{\downarrow}}\frac{\Gamma_s^{\downarrow}}{d}=2\pi\frac{\Gamma_s^{\downarrow}}{d}(F_{NN}^{w})^2\ , \tag{4.7}$$

which we have rewritten in terms of the weak strength constant and of a large factor $2\pi\Gamma_s^{\downarrow}/d$, which stands for dynamical enhancement. Its order of magnitude is $\Gamma_s^{\downarrow}/d\sim\Lambda$, i.e., the number of configurations effectively mixed by the residual interaction. Thus this factor turns out to be the same as Blin-Stoyle's "number enhancement" [43].

### B. Introduction of the interaction lifetime

In Appendix B, we show that the two-point function $Q$ of Sec. III B is a well defined quantity of general scattering theory. Using only fundamental requirements such as causality, unitarity, symmetry, and stationarity, one gets an appealing interpretation and additionally a completely independent check of the results in Sec. III B (which first were obtained by the algebraic methods of Verbaarschot *et al.* [11]):

$$\begin{aligned}\overline{Q_{pp}}&=i\hbar\overline{\left[S^{+}\frac{\partial}{\partial E}(S^{+})^{*}\right]_{pp}}\\&=i\hbar\frac{\partial}{\partial\epsilon}\overline{[S^{+}(E_1)(S^{+})^{*}(E_2)]_{pp}}|_{\epsilon=E_2-E_1=0}\ .\end{aligned} \tag{4.8}$$

Remember that the superscript + denotes parity, not Hermitian conjugation. The quantity under the average bar on the right-hand side of the first equation has precisely the form [44,45] of the so-called "collision lifetime" or "interaction time," as we shall call it. Its meaning is that of the delay time, which a particle passing through the interaction region is suffering with the interaction switched *on* in comparison to the delay with the interaction switched *off*. A deduction and discussion of the properties of this quantity can be found in the above-mentioned references; we now turn to the interpretation.

The variance of the parity forbidden scattering matrix experiments, according to Eqs. (3.14) and (3.15), is given by the product of the average interaction lifetimes in entrance and exit channel. In order to give an expression for $\overline{|S^{PV}|^2}$, which is purely based on the different time scales occurring in a nuclear reaction, we introduce the following quantities: the *recurrence* time ([46], Eq. (7.10)) $h/d$ and, also in accordance with the current understanding [47], the *mixing* time $h/\Gamma_w^{\downarrow}$. The latter one can be interpreted as the time constant of the relaxation of an originally pure parity state to a parity mixture [46]. Henceforth, with the set of renamings

$$\sqrt{\overline{Q_{pp}}\,\overline{Q_{mm}}}=T_{\rm int},\quad\frac{h}{d}=T_{\rm rec},\quad\frac{\hbar}{\Gamma_w^{\downarrow}}=T_{\rm mix} \tag{4.9}$$

we have the following suggestive formula

$$\overline{|S_{pm}^{PV}|^2}=\frac{T_{\rm int}^2}{T_{\rm mix}T_{\rm rec}}\ . \tag{4.10}$$

Note the distinction between average interaction time and average compound nucleus lifetime: the former one is *not* merely proportional to $1/\Gamma$, i.e., the reciprocal linewidth. Quite surprisingly it even can be proportional to $1/d$, i.e., the reciprocal level distance. This can be shown with the simple model of equivalent channels, where all transmission coefficients are equal $T_c=T$. The interaction time in a given channel then can be expressed by a channel sum, which, in turn, can be evaluated by virtue of unitarity [cf. Eq. (3.7)]:

$$\begin{aligned}\overline{Q_{pp}}&=\frac{1}{N^{+}}\sum_{p'}\overline{Q_{p'p'}}\\&=\frac{2\pi\hbar}{N^{+}}\sum_{p'}\overline{[(V^{+})^{T}G^{+}(G^{+})^{*}V^{+}]_{p'p'}}\\&=\frac{2\pi\hbar}{N^{+}}\overline{\mathrm{Tr}[G^{+}V^{+}(V^{+})^{T}(G^{+})^{*}]}\\&=\frac{2\pi\hbar}{N^{+}}\overline{\mathrm{Tr}[-(1/\pi)\mathrm{Im}(G^{+})]}=2\pi\hbar/(N^{+}d^{+})\ .\end{aligned} \tag{4.11}$$

Note that this is (within the GOE formalism) a rederivation of a result found by Lyuboshits in a somewhat more heuristic way [49,50].

*Interpretation.* The parity violating cross section is given by the variance of the parity violating Hamiltonian elements and the product of interaction times in the entrance and exit channel. The longer these interaction times, the larger is the expected value of the parity violation effect. Due to the fact that we deal with average delay times and not common lifetimes, both the average width and the average distance of the resonances are involved: on the one hand, the delay time *on* resonance is $1/\Gamma$ and *off* resonance $1/d$ (i.e., negligible for $d\ll\Gamma$, the "weak absorption case"); on the other hand, the probability to hit a resonance in channel $c$ is proportional to $\Gamma_c/d$ (where $\Gamma_c$ is the partial width). The total effect depends on both the absolute value of $\Gamma$ and on the ratio $\Gamma_c/d$. In this sense the lifetime enhancement incorporates the resonance, dynamical, and kinematical factors of Sec. II A.

### C. External mixing

So far we have not considered the presence of weak forces in the coupling $V$. This deserves a justification. The most general form of the coupling would (if $T$ invariance holds) look like

$$V=\begin{pmatrix}V^{+}&\emptyset\\\emptyset&V^{-}\end{pmatrix}+\begin{pmatrix}\emptyset&V^{+-}\\V^{-+}&\emptyset\end{pmatrix}\ . \tag{4.12}$$

The occurrence of the parity violating part, e.g., $V^{+-}$, has two effects, which can be located in the basic equations for the $S$ matrix: for the $V$ multiplying $G$ in Eq. (3.4), they lead to a parity forbidden transmission into the compound nucleus, i.e., the coupling of a channel with given parity to a resonance with the opposite parity; for the $V$ occurring in $G$ through the decay matrix $W=i\pi VV^{T}$, see Eq. (3.5), they lead to an external mixing. By virtue of orthogonal invariance these two effects may be cast into the following forms.

*First effect.* The direct parity violating coupling leads to parity forbidden transmission coefficients, which connect a channel of given, say negative, parity to resonances with the opposite parity. Consider the scalar products $\mathbf{V}_a \circ \mathbf{V}_b$ of the coupling vectors $\mathbf{V}_p^T=((\mathbf{V}_p^+)^T,(\mathbf{V}_p^{+-})^T)$ [where $a$, $b$ denote any channel of positive ($p$) or negative ($m$) parity]. For $a \neq b$ they can be neglected by virtue of the same random interference argument, which explains Eq. (3.6). Turning to $a=b=p$ (similarly for $a=b=m$) and assuming $(1/\Lambda^-)|\mathbf{V}_p^{+-}|^2 \sim (1/\Lambda^+)|\mathbf{V}_p^+|^2 (F_{NN}^w)^2$ (note the squares), the coupling constants as defined in Eq. (3.22) will contain a parity forbidden part

$$x_p^{+-} \sim (F_{NN}^w)^2 x_p^+ = (F_{NN}^w)^2 \pi^2 |\mathbf{V}_p^+|^2 / \Lambda^+ d^+ ,$$

where $x_p^+$ is the parity allowed part. As long as the transmision coefficient corresponding to the latter [see Eq. (3.21)] fulfills $T_p^+ \sim x_p^+$, i.e., $x_p^+ \lesssim 1$, we will also have

$$T_m^{+-} \sim (F_{NN}^w)^2 T_m^- . \tag{4.13}$$

Now, cross sections are continuous functions of the transmission coefficients, which have, according to Verbaarschot *et al.* [11], the general form of a corrected Hauser-Feshbach expression

$$\sigma_{pp'} = T_p T_{p'} (\textstyle\sum T_c)^{-1} K(T_p, T_{p'}, \ldots) ,$$

where $K$ is a correction function of the order of unity. In the presence of parity-violating transmission coefficients of the form (4.13) one has

$$\sigma_{mp'}^{PV} \sim \frac{T_m T_{p'}}{\sum T_c} (F_{NN}^w)^2 . \tag{4.14}$$

In the case of slow neutron scattering, $m$ is a $p$-wave channel, $p$ is the $s$-wave channel and $\sigma_m^t = \sum_{m'} \sigma_{mm'} \sim T_m$. Then, we have a ratio $\sigma_{mp}^{PV}/\sigma_m^t \propto T_p (\sum T_c)^{-1} (F_{NN}^w)^2$, which has a multiplying factor even smaller than 1, meaning hindrance, not enhancement. An interesting, albeit rather unrealistic, situation can occur if $T_p^+ \sim (x_p^+)^{-1}$, i.e., if $x_p^+ \gg 1$: then, $T_p^{+-} \sim T_p^+$ is possible. Consider the function $T(x)=4x/(1+x)^2$ connecting coupling parameter and transmission coefficient [see Eq. (3.21)] and write $T_c = T(x_c)$. Equating $T(x_p^+) = T(x_p^+ (F_{NN}^w)^2) \sim T_p^{+-}$ yields $x_p^+ \sim (F_{NN}^w)^{-1} \sim 10^7$, i.e., for such an extremely absorptive channel, the strong and the parity forbidden transmission coefficient may be comparable. The reason for this surprising behavior is that a wave packet gets reflected rather than transmitted at *any* large change of the potential, even when it is an absorptive well; if, however, the incoming wave in addition couples weakly to the resonances of opposite parity, these are seen as a much shallower well, which is much easier to penetrate. [A similar consideration shows, that for $x_p^+ \sim (F_{NN}^w)^{-2} \sim 10^{14}$, one could even have $T_p^{+-} \sim 1 \gg T_p^+$.]

*Second effect.* The parity-violating blocks of the decay matrix have the form

$$W^{+-} = i\pi [V^+ (V^{+-})^T + V^{+-} (V^-)^T] . \tag{4.15}$$

This matrix plays exactly the same role as an arbitrary and fixed $H^{+-}$ in Sec. IV A. We already know that the GOE then averages out an orthogonal invariant [cf. Eq. (4.4)]:

$$(w^{\text{ext}})^2 = \frac{1}{\Lambda^+ \Lambda^-} \text{Tr}[W^{+-} (W^{+-})^T] , \tag{4.16}$$

which in closest analogy to $w^2$ of $H^w$ leads to an *external* spreading width. It can be written (again in the weak absorption limit) as

$$\frac{\Gamma^{\downarrow,\text{ext}}}{d} \overset{\text{def}}{=} 2\pi \frac{(w^{\text{ext}})^2}{d} = \frac{2}{\pi} (F_{NN}^w)^2 \left[ \sum (x_p^+)^2 + \sum (x_m^-)^2 \right] . \tag{4.17}$$

This has to be compared with the corresponding expression (4.7) for the *internal* spreading width, thus revealing that there is no *a priori* reason to neglect the external coupling in comparison to the internal one. On the contrary, the two effects become equal if the sum of the squared coupling parameters [the term in large parentheses in (4.17)] becomes comparable to $2\pi\Gamma_s^{\downarrow}/d$, which may happen in a region of extremely overlapping resonances.

*Interpretation.* A parity forbidden part in the coupling $V$ leads to two effects. First, of parity violating transmission coefficients of the order of magnitude $(F_{NN}^w)^2 \sim 10^{-14}$ occur. These transmission coefficients enter parametrically in $\bar{S}$ and $\overline{|S|^2}$ and produce effects of the same order of magnitude. There is no lifetime enhancement: the perturbation acts only during a "penetration time," which is much shorter than the average interaction time. Second, a parity forbidden spreading width occurs, which enters multiplicatively before $Q_{pp}\, Q_{mm}$. It is (as the internal spreading width) of second order in the perturbation, but additionally of fourth order in the coupling to the channels. Thus this effect does profit, on the one hand, from lifetime enhancement, but can be, on the other hand, neglected in the case of isolated resonances.

## V. A PREREQUISITE: INCLUSION OF FINITE ENERGY RESOLUTION

Up to now it was assumed that all resonances and fluctuations in excitation or transmission functions may be measured with arbitrarily precise resolution, i.e., with their line width being unaltered by any influence of the experimental setup. In Sec. IV B we have pointed out that all parity nonconserving observables decisively depend on the lifetime, i.e., the inverse linewidth. Hence, it should be intuitively understandable that any form of line broadening leads to a lowering of the measureable effect. An answer to the question about the influence of finite energy resolution is thus an indispensible prerequisite to the question of feasibility of symmetry violation experiments with energy averaging.

Our formalism allows one to answer this question. Finite energy resolution means to measure a signal $f(E)$ not only at one energy $E$, but as a summation of the form

$$f^{E \pm \Delta E} = \int f(E') r(E - E') dE' , \tag{5.1}$$

i.e., the convolution with the experimental resolution function $r$ of given halfwidth $\Delta E$. We now assume the function $f$ to be our two-point function, $\overline{L_p}=d^+\overline{Q_{pp}}/h$, cf. Eq. (3.24). Consider $\overline{Q_{pp}}$ in the form (3.15), but with $G$ and $G^*$ taken at two different energies $E_1$, $E_2$:

$$\overline{L_p(E_1-E_2)}\equiv\frac{d^+}{h}\overline{Q_{pp}(E_1-E_2)}$$
$$\equiv 2\pi d^+\overline{\{(V^+)^T G^+(E_1)[G^+(E_2)]^+V^+\}_{pp}}\ . \tag{5.2}$$

The fact that GOE averaged two-point functions depend on the difference $\epsilon=E_2-E_1$ alone is shown in Ref. [11]; more precisely it occurs as a "Fourier" factor in the final integrations. These are, in general [11], three-dimensional in the arguments $\lambda_1$, $\lambda_1$, $\lambda$ and the energy dependence reads as $\exp[-i\pi(\epsilon/d)(\lambda_1+\lambda_2+2\lambda)]$; in the limit of isolated resonances [34], there is only one final integration in $x$ with a "Fourier" factor $\exp[-i\pi(\epsilon/d)x]$. Some of the following considerations apply to both the general and the limiting cases, and we shall use a common abbreviation $\theta=\pi(\lambda_1+\lambda_2+2\lambda)/d$ or $\theta=\pi x/d$, respectively.

We now imagine an "experimental measurement" of $\overline{L_p}$ to consist of two steps. First, a measuring (5.2) with finite resolution,

$$\overline{L_p(\epsilon)}^{E\pm\Delta E}=\int_{-\infty}^{\infty}\int_{-\infty}^{\infty}\overline{L_p(E_2'-E_1')}r(E_2'-E_2)$$
$$\times r(E_1'-E_1)dE_2'dE_1'\ . \tag{5.3}$$

Note that we have to perform a convolution over both $E_1$ and $E_2$, because both points of the two-point function are "smeared out" experimentally. Second, extrapolating to the limit $\epsilon=0$,

$$\overline{L_p}^{E\pm\Delta E}=\lim_{E_1\to E_2}\overline{L_p(\epsilon)}^{E\pm\Delta E}\ . \tag{5.4}$$

It is shown in Appendix C that the Fourier form of the energy dependence leads to a simple recipe: $\overline{L_p}^{E\pm\Delta E}$ is obtained from $\overline{L_p}$ by the following substitution:

$$\prod\to\prod\tilde{r}^2(\theta)\ , \tag{5.5}$$

where $\prod$ is either the product function of the threefold integration (3.18) in the general case or of the single integration (3.28) in the isolated resonance case, and $\tilde{r}(\theta)$ is the Fourier transform of the resolution function:

$$\tilde{r}(\theta)=\int_{-\infty}^{\infty}e^{i\theta}r(E)dE\ . \tag{5.6}$$

We now make two specific choices for $r(\theta)$ and additionally assume the "lumping approximation." Then we obtain an even simpler recipe than (5.5) for the substitution in Eq. (3.26):

$$r_L(\epsilon)=\frac{\Delta E/\pi}{\epsilon^2+(\Delta E)^2}\ ,$$
$$e^{-(\lambda_1+\lambda_2+2\lambda)T_L/2}\to e^{-(\lambda_1+\lambda_2+2\lambda)T_L/2}e^{-(\lambda_1+\lambda_2+2\lambda)2\pi\Delta E/d}\ , \tag{5.7}$$
$$r_G(\epsilon)=\frac{e^{-\epsilon^2/2(\Delta E)^2}}{\sqrt{2\pi(\Delta E)^2}}\ ,$$
$$e^{-(\lambda_1+\lambda_2+2\lambda)T_L/2}\to e^{-(\lambda_1+\lambda_2+2\lambda)T_L/2}e^{-(\lambda_1+\lambda_2+2\lambda)^2(\pi\Delta E/d)^2}\ ,$$

for a Lorentzian and Gaussian resolution function, respectively. The Lorentzian case now allows an intuitively very appealing interpretation: the sum of transmission coefficients $T_L$ of the lumped channels has to be replaced by $T_L+4\pi\Delta E/d$ or the corresponding linewidth $\Gamma_L$ by $\Gamma_L+2\Delta E$. (The additional factor of 2 here comes from the fact that we have to apply the resolution function two times, i.e., we have a double convolution.) If we implement the replacements (5.7) in the combined limit of weak absorption and lumping of all channels [see Eq. (3.30)], we obtain analytical results for both the Lorentzian and Gaussian cases. Setting

$$T_R^\pi=2\pi\frac{\Delta E}{d^\pi},\quad R_\pi=\frac{T_L^\pi}{2T_R^\pi} \tag{5.8}$$

the result for a Lorentzian weighting is

$$\overline{L_p}^{E\pm\Delta E}=\frac{T_p}{T_L^+}(1+R_+^{-1})^{-1}$$
$$\to\frac{T_p}{2T_R^+}\quad\text{for } T_R^+\gg T_L^+ \tag{5.9}$$

and for a Gaussian weighting one obtains

$$\overline{L_p}^{E\pm\Delta E}=\frac{T_p}{T_L^+}\sqrt{\pi}R_+e^{R_+^2}\mathrm{erfc}(R_+)$$
$$\to\frac{T_p}{(2/\sqrt{\pi})T_R^+}\quad\text{for } T_R^+\gg T_L^+\ . \tag{5.10}$$

The first forms of Eqs. (5.9) and (5.10) for $T_R^+\to 0$ (or $R_+\to\infty$) lead back to the old results without resolution correction, as it should be (the function $\sqrt{\pi}x\exp(x^2)\mathrm{erfc}(x)$ tends to 1 with $x\to\infty$; see Ref. [36], Eq. 7.1.23. The second form of (5.10) was obtained with help of Eq. (7.2.7) of Ref. [36]. The ratio $(2/\sqrt{\pi})^{-1}:2^{-1}\approx 1.8$ of the Gaussian to the Lorentzian case reflects the slower falloff and hence stronger "smearing" of the latter one.

Up to now we had assumed that the measured quantity, i.e., the function $f$ of Eq. (5.1) is $L_p(E)$, which means that $L_p(E)$ and $L_m(E)$ are measured *separately*. But in transmission experiments, one actually measures the product $L_p(E)L_m(E)$ i.e., one is dealing with a *correlated* measurement. This leads to a complication, mathematically to be stated as follows:

$$\overline{L_pL_m}^{E\pm\Delta E}=\int\int\overline{L_p(\epsilon')L_m(\epsilon')}r(E_1-E_1')$$
$$\times r(E_2-E_2')dE_2'dE_1'\ , \tag{5.11}$$

where $\epsilon' = E_2' - E_1'$. Technically, this double convolution generally will lead to an integration, where the arguments of $L_p$ and $L_m$ are no longer independent. In the general case, this entanglement of arguments leads to an unpleasant sixfold integration. Only in the case of Lorentzian resolution one obtains (see Appendix C)

$$\overline{L_p L_m}^{E\pm\Delta E} = \overline{L_p}^{E\pm\Delta E}\,\overline{L_m}^{E\pm\Delta E} . \tag{5.12}$$

In the case of Gaussian resolution, this identity does not hold, but we can get a simple analytical form under the same assumptions as before (weak absorption, lumping of all channels). It is (see Appendix C)

$$\overline{L_p L_m}^{E+\Delta E} = \frac{T_p T_m}{T_L^+ T_L^-}\sqrt{\pi}\frac{R_+ \cdot R_-}{R_+ - R_-} \times [e^{R^2}-\mathrm{erfc}(R_-)-e^{R_+^2}\mathrm{erfc}(R_+)] . \tag{5.13}$$

In low-energy neutron scattering, we often have the physical situation where $\Gamma_{\mathrm{tot}}^+ \approx \Gamma_{\mathrm{tot}}^- \overset{\mathrm{def}}{=} \Gamma_{\mathrm{tot}}$, i.e., $R_+ \approx R_- \overset{\mathrm{def}}{=} R$. In this limit, Eq. (5.13) can be rewritten as a derivative and one obtains (see Appendix C)

$$\overline{L_p L_m}^{E+\Delta E} = \frac{T_p T_m}{T_L^+ T_L^-} 2R^2[1-\sqrt{\pi}\mathrm{Re}^{R^2}\mathrm{erfc}(R)] . \tag{5.14}$$

Both (5.13) and (5.14) lead back to the old result $\overline{L_p}\,\overline{L_m}$ for the case of ideal resolution, i.e., $\Delta E \to 0$.

Finally, we again consider $\Delta E \gg \Gamma_L^{\pm}$, i.e., the case of very poor resolution. (Note, that this is still compatible with $D \gg \Delta E$.) Then, $T_L^\pi / 2T_R^\pi \to 0$ and in this limit Eq. (5.13) becomes (by means of Eq. 7.2.7 of Ref. [36]):

$$\overline{L_p L_m}^{E+\Delta E} = \frac{T_p T_m}{2T_R^+ T_R^-} . \tag{5.15}$$

Note, that the ratio of (5.15) (correlated measurement) to the product $\overline{L_p}^{E+\Delta E}\,\overline{L_m}^{E+\Delta E}$ given by (5.10) (separate measurement) is

$$\overline{L_p L_m}^{E+\Delta E} / \overline{L_p}^{E+\Delta E}\,\overline{L_m}^{E+\Delta E} = \frac{2}{\pi} \approx 0.63 < 1 . \tag{5.16}$$

This means that a correlated measurement with Gaussian resolution function reduces the measurable effect more than a separate measurement and can be understood as follows: consider $\tilde{\epsilon} = \frac{1}{2}(E_2^+ - E_1^+ + E_2^- - E_1^-)$ where all arguments shall fluctuate with the same variance $\Delta E$. If all arguments are independent (separate measurement) $\tilde{\epsilon}_{\mathrm{rms}}^{\mathrm{sep}} = \frac{1}{2}\sqrt{4\Delta E^2} = \Delta E$. If, however, $E_2^+ = E_2^-$ and $E_1^+ = E_1^-$, one gets $\tilde{\epsilon}_{\mathrm{rms}}^{\mathrm{corr}} = \frac{1}{2}\sqrt{8\Delta E^2} = \sqrt{2}\Delta E$. For both cases, one has to replace $\Gamma_L^\pi$ in Eq. (3.31) by $\tilde{\epsilon}_{\mathrm{rms}}$ in the limit of very poor resolution and thus one can estimate

$$\overline{L_p L_m}^{E+\Delta E} / \overline{L_p}^{E+\Delta E}\,\overline{L_m}^{E+\Delta E} \approx \frac{1/\tilde{\epsilon}_{\mathrm{rms}}^{\mathrm{corr}}}{1/\tilde{\epsilon}_{\mathrm{rms}}^{\mathrm{sep}}} = \frac{1}{\sqrt{2}} \approx 0.71 , \tag{5.17}$$

which is not very different from (5.16).

## VI. APPLICATION TO NEUTRON OPTICAL EXPERIMENTS

This type of experiments entails two gratifying features from the theoretical point of view: First, the data pool is one of the best available in all nuclear physics; second, the physical situation is such that the approximations of Sec. III C can be applied.

### A. Transmission coefficients and level densities

For low-energy neutron scattering, only two types of basically different channels are open, namely neutron and $\gamma$ channels, and all these channels are weakly absorbed. This limit means that the transmission coefficients, as defined via Eqs. (3.21) and (3.22), are connected to the average widths as follows:

$$T_a \approx 4x_a = 2\pi\frac{\Gamma_a}{d^{J\pi}} (a = \alpha, l, i, j, I, J, M, \pi) . \tag{6.1}$$

Additionally, we can restrict ourselves to $l = 0, 1$ ($p$-wave approximation). From the full channel index $a$ the labels $i, I$ (projectile spin, target spin) are fixed by the chosen type of experiment. The transmission coefficients and the scattering matrix will not depend on the label $M$ due to axial symmetry. Both the partial widths and level distances may depend on $l, j, J$. So we shall write $T_c = T_{\alpha,l,j,J,\pi}$. What is found in the literature [51,52] are the so-called "reduced strength functions" $S_0$, $S_1$, $S_{\gamma 0}$, $S_{\gamma 1}$ for neutrons and gammas and different partial waves $l$ ($l = 0, 1$) which are weighted sums over the quantum numbers $j$ and $J$. For $l = 1$ they contain contributions of different $j$ and for $I \neq 0$ also of different $J$. How to get "quantum number pure" transmission coefficients $T_a$ (with $j$, $J$ given) from the above strength functions is described in Appendix D. Droppping the redundant $\pi$ (because, for a given target, parity is fixed by the angular momentum of the incoming neutron) the result for the neutron channel reads as

$$\begin{aligned} T_{n,0,\frac{1}{2},J} &= T_{n0}(E) = T_{n0}(1)\epsilon^{1/2} , \\ T_{n,1,\frac{1}{2},J} &= T_{n1}(E) = T_{n1}(1)\epsilon^{3/2} , \end{aligned} \tag{6.2}$$

where $\epsilon$ is the energy in eV and

$$\begin{aligned} T_{n0}(1) &= 2\pi S_0 , \\ T_{n1}(1) &= 2\pi S_1 \rho^2 10^{-6} , \end{aligned} \tag{6.3}$$

where $\rho = R/4.55$ fm is the nuclear radius of the target nucleus divided by the de Broglie wavelength of a neutron with the reference energy 1 eV. Note, that we now dropped also the labels $j$, $J$ because the resulting transmission coefficients do not depend on it. This is the result of an additional assumption in our extraction procedure, corresponding to an optical model without spin-orbit coupling.

The result for the $\gamma$ channels is as follows (it is to be understood that $\pi = +1$ for $s$-wave resonances, i.e., when $l = 0$; and that $\pi = -1$ for $p$-wave resonances, i.e., when $l = 1$):

$$T_{\gamma,J,\pi}=2\pi S_{\gamma l}/e_{Jl} \tag{6.4}$$

with an extraction factor $e_{Jl}$ given by the level densities for different $J$,

$$e_{Jl}=\sum_{|I-l-1/2|\le J'}^{I+l+1/2}\frac{\rho_{J'}}{\rho_J} \tag{6.5}$$

with

$$\rho_J=(2J+1)e^{-(J+1/2)^2/2\sigma^2}\ , \tag{6.6}$$

which is the spin-dependent part of the usual [53–55] level density formulas: $\sigma$ is the spin cutoff parameter, for which we have taken a semiempirical fit formula [55]. The extraction factor is $\ge 1$, i.e., $T_{\gamma J\pi}\le 2\pi S_{\gamma l}$; this is plausible, because the $S_{\gamma l}$ count the coupling of levels for more than one value of $J$.

In distinction to the neutron transmission coefficients those for the $\gamma$ channels are labeled by the total angular momentum $J$. They depend on $J$ because the level densities do so. We now turn to these.

Again, the literature gives level distances $D_0$, $D_1$ labeled by $l$ only; for target spins $I\neq 0$ this means grouping together levels with different $J$. What we need are again quantum number pure quantities $d^{J\pi}$. The connection to the measured quantities can be established (under reasonable assumptions; see Appendix C):

$$d^{J\pi}=D_l\,e_{Jl}\ , \tag{6.7}$$

with the extraction factor from (6.5). It is clear that $d^{J\pi}\ge D_l$, because for $D_l$ more levels are taken into account, thus yielding smaller level distances.

By now we have a set of input parameters sufficient for the numerical evaluation of lifetimes and parity forbidden cross sections for concrete nuclei.

### B. Numerical results

It should be emphasized that the $\gamma$-transmission coefficients defined in the last section are still not pertaining to one scattering channel; rather they are a sum

$$T_{\gamma,J,\pi}=\sum_{g}^{N_\gamma}T_{g,J,\pi}\ , \tag{6.8}$$

where $g$ runs over $\gamma$ rays of different energies and multipolarity. Fortunately, the number $N_\gamma$ of these channels is very high, so that the condition for the "lumping approximation" (3.26) holds; thus the important parameter is precisely the sum of transmission coefficients (5.4) and not the individual transmission coefficients.

We are now in the position to give numerical results for both the average interaction times and parity violation observables. The rms values of the following observables are equal to each other:

$$\Delta\overset{\text{def}}{=}\Delta A_{\text{opt}}=\Delta P_{\text{opt}}=\Delta\Phi_{\text{opt}}\overset{\text{def}}{=}(\overline{\Phi_{\text{opt}}^2}-\overline{\Phi_{\text{opt}}}^2)^{1/2}=(\overline{\Phi_{\text{opt}}^2})^{1/2}\ , \tag{6.9}$$

(the definitions of $\Delta A_{\text{opt}}$, $\Delta\Phi_{\text{opt}}$ and the vanishing of their mean values hold analogously) and are given by

$$\Delta=4\pi\frac{1}{\sigma^t k^2}\left\{\frac{1}{2}\left[\left(\frac{I+1}{I+\frac{1}{2}}\right)^2\overline{|S_{10}^{I+1/2}|^2}+\left(\frac{I}{I+\frac{1}{2}}\right)^2\overline{|S_{10}^{I-1/2}|^2}\right]\right\}^{1/2} \tag{6.10}$$

with the parity forbidden cross section

$$\overline{|S_{10}^{J}|^2}=2\pi\frac{\Gamma^{\downarrow}}{d^J}\bar{L}_{J0}\bar{L}_{J1}\ , \tag{6.11}$$

and the collision times [in the approximation (3.29)]

$$\bar{L}_{Jl}=1-xe^{x^2/2}\int_x^\infty e^{-x'^2/2}dx',\quad x=\sqrt{T_L^\pi/T_{nl}}\ . \tag{6.12}$$

Here, the lumped transmission coefficient is $T_L^+=T_{\gamma,J,+}$ for the $s$-wave channel and $T_L^-=T_{\gamma,J,-}+T_{n,1,\frac{3}{2},J}$ for the $p$-wave channel.

The spreading width is given in Sec. IV A 2. We made the simplifying assumption that $\Gamma_w^{\downarrow}$ does not depend on $J$. If there are variations of $\Gamma_w^{\downarrow}$ with spin, energy, and target nucleus, they are at present unknown; our ansatz aims to display the dependence of parity violation observables on known average quantities (namely, $d$'s and $T$'s). The purpose of doing so is twofold: (i) hints for possible favorable experiments; (ii) verification of the estimated value of $\Gamma_w^{\downarrow}$ from given experiments.

For the total cross sections we take the (slow neutron) approximation ([51], Eq. (39))

$$\sigma^t=\sigma^{\text{pot}}+\sigma^{\text{abs},s}=4\pi(R')^2+\pi T_{n0}/k^2\ . \tag{6.13}$$

This is the average cross-section including potential scattering (equivalent scattering radius $R'$, which we have taken from Mughabghab *et al.* [51,52]; when the value is not tabulated, we interpolated it from the neighboring nuclei or the eye-guide curve in Fig. 2, Vol. 1B of Ref. [52]) and $s$-wave absorption. The general behavior of the quantity $\Delta$ with energy is as follows: the increase at low energies is due to the increasing penetrability of the $p$-waves; the subsequent decrease at higher energies comes from the decrease of lifetimes.

We give for a series of nuclei the following results: First, in Fig. 2 the rms effect as a function of energy (from the whole set of nuclei, we have displayed those with the most complete set of input data, cf. Tables II and III); second, in Fig. 3 the rms $\Delta$ effect at 1 eV as a function of mass number; third, in Table I the energy $E_m=E(\max)$ where the maximum effect is found, the corresponding target thickness, some factors dedicated to in-

terpretation (and explained in the following section), and the rms $\Delta$ value at $E_m$. [For the calculation of the target thickness we took *elemental* densities (uncorrected for isotopic dependence) from Ref. [56]; for the following elements, we had to make a choice of the modification: Se (grey), Rb (solid), Sn (grey), Sm ($\alpha$); see Ref. [56] for notation.]

### C. Discussion

For the sake of interpretation, we will discuss our result in the form of the following approximations, which are crude, but clearly exhibit the main influences on the total effect:

$$\Delta \sim 4\left[\frac{T_{n1}}{T_{n0}}\right]^{1/2}\left[4\pi\frac{\Gamma_s^{\downarrow}}{d^J}\right]^{1/2}(T_L^+T_L^-)^{-1/2}F_{NN}^w$$
$$\approx 4\left[\frac{T_{n1}}{T_{n0}}\right]^{1/2}\left[2\frac{\Gamma_s^{\downarrow}}{\Gamma_{\gamma,J,-}}\right]^{1/2}\left[2\pi\frac{\Gamma_{\text{tot},J,+}}{d^{J,+}}\right]^{-1/2}F_{NN}^w . \tag{6.14}$$

In the first line, we have assumed $I=0$, (i.e., $J=\frac{1}{2}$), Eq. (4.7) for $\Gamma_w^{\downarrow}$, Eq. (3.31) for $\overline{L_a}$, and additionally

$$4\pi/\sigma^t k^2=(4/T_0)(1+\sigma^{\text{pot}}/\sigma^{\text{abs},s})^{-1}\sim 4/T_0 ,$$

which is roughly true, because $\sigma^{\text{pot}}/\sigma^{\text{abs},s}\lesssim 1$ (see the end of this subsection). In the second line we furthermore assumed

$$T_L^+\sim\sum T_{c,J,+}=2\pi\Gamma_{\text{tot},J,+}/d^{J+}$$

and

$$T_L^-\approx T_{\gamma,J,-}=2\pi\Gamma_{\gamma,J,-}/d^{J-}$$

(the first approximation is crude, the second accurate; see end of paragraph). We give two alternative forms, depending on what is considered as basic quantities. In both forms, the three square root factors correspond very closely to the three enhancement mechanisms explained in Sec. II.

The factor $V_{\text{kin}}=\sqrt{T_{n1}/T_{n0}}$ measures the ratio of penetrabilities of $s$ and $p$ waves and corresponds to the kinematical factor explained in Sec. II. It is dominating the $A$ dependence of the total effect, as one can see from Fig. 3: there, we compare (at 1 eV) $\Delta$—the "parity forbidden strength function"—with $V_{\text{kin}}$ (essentially given by the ratio of neutron strength functions) and see that it follows the qualitative features of the latter. These features are well explained by the optical model, cf. Figs. 3 and 4 of Ref. [52]: the minimum at $A=50$–$60$ comes from the $3S$ shell, the maximum at $A=90$–$120$ from the $3P$ shell, the minimum at $A=150$–$190$ from the $4S$ shell, and the indication of a maximum around $A\approx 240$ coincides with the $4P$ shell. There is an indication for the double-well structure of the $4S$ minimum, as well as for a double-humped structure of the $3P$ maximum. We emphasize that the curves for $\Delta(E_m)$, with $E_m$ being the energy where the maximal effect is found, can essentially be obtained from those at 1 eV by a parallel shift by one order of magnitude up, i.e., their energy dependence is basi-

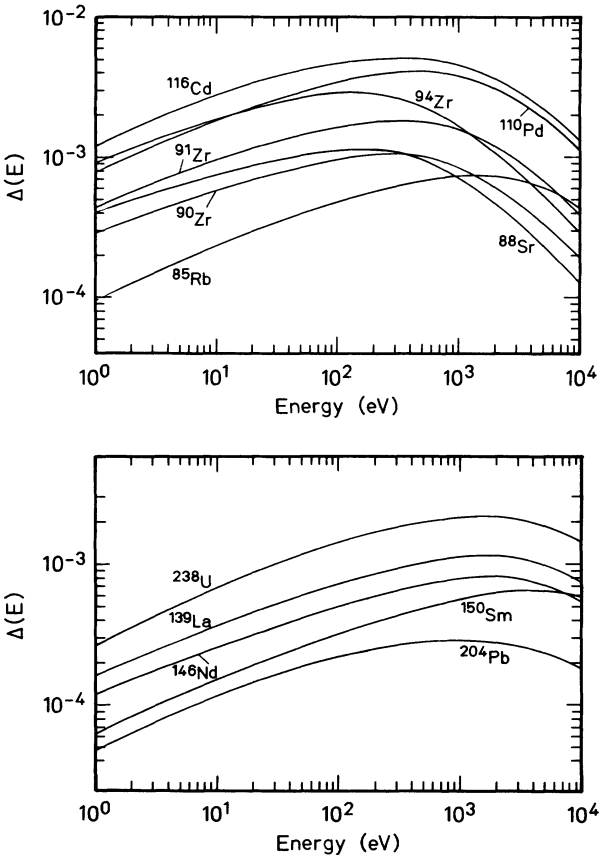


FIG. 2. Energy dependence of $\Delta$ [defined in Eq. (6.10)] for various targets; see Sec. VI C. Upper part, $A\leq 120$; lower part, $A>120$.

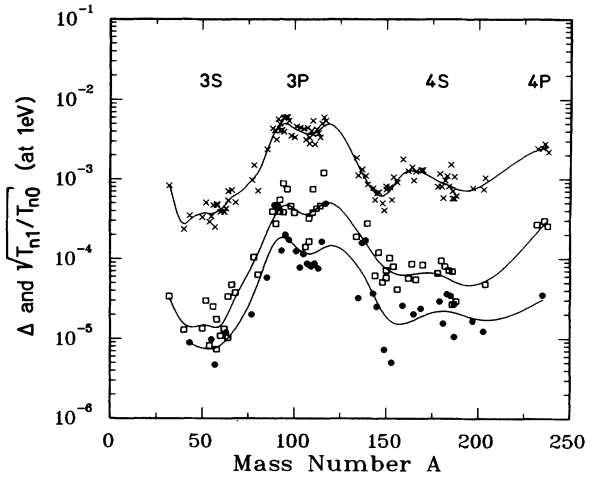


FIG. 3. "Parity forbidden strength function" $\Delta$ and kinematic suppression factor $V_{\text{kin}}$ (ratio of $s$- and $p$-wave neutron strength functions) at $E=1$ eV (□, $\Delta$ for even nuclei; ●, $\Delta$ for odd nuclei; ×, $V_{\text{kin}}=\sqrt{T_{n1}/T_{n0}}$). The solid curves are guides for the eye (obtained by spline interpolation) to the calculated data points. For further discussion see Sec. VI C.

TABLE I. Parity forbidden effect and determining factors at $E = E_{max}$ for various target nuclei, see Sec. VI C. The delay time $Q_{pp}$ pertains to the neutron channel $p$ with quantum numbers $l = 0$, $j = \frac{1}{2}$, $J = I + \frac{1}{2}$.

| Nucleus | $E_m$ (eV) | $l$ (cm) | $V_{kin}$ ($10^{-1}$) | $V_{time}$ | $V_{dyn}$ | $V_{res}$ | $V_{tot}$ | $\overline{Q_{pp}}$ ($10^{-20}$ s) | $\Delta$ ($10^{-4}$) |
|---|---|---|---|---|---|---|---|---|---|
| $^{32}$S | 1400 | 5.40 | 0.31 | 2200 | 30 | 7.6 | 510 | 6 | 2.00 |
| $^{40}$Ca | 1600 | 2.50 | 0.09 | 5000 | 35 | 3.5 | 160 | 9 | 0.74 |
| $^{43}$Ca | 4500 | 4.40 | 0.23 | 3400 | 76 | 2.7 | 210 | 40 | 0.69 |
| $^{50}$Cr | 2200 | 0.67 | 0.16 | 4900 | 66 | 3.1 | 230 | 25 | 0.94 |
| $^{52}$Cr | 660 | 0.56 | 0.13 | 5400 | 37 | 5.0 | 350 | 9 | 1.50 |
| $^{54}$Fe | 1700 | 0.26 | 0.12 | 4700 | 67 | 2.1 | 120 | 29 | 0.52 |
| $^{55}$Mn | 3600 | 0.84 | 0.20 | 4700 | 110 | 2.6 | 250 | 71 | 0.73 |
| $^{56}$Fe | 1400 | 0.72 | 0.18 | 5400 | 64 | 4.0 | 390 | 22 | 1.40 |
| $^{57}$Fe | 5700 | 0.89 | 0.19 | 3400 | 89 | 2.2 | 140 | 45 | 0.43 |
| $^{58}$Fe | 880 | 0.43 | 0.14 | 4600 | 45 | 3.8 | 250 | 11 | 0.93 |
| $^{58}$Ni | 3400 | 0.79 | 0.28 | 1800 | 67 | 3.1 | 160 | 26 | 0.56 |
| $^{60}$Ni | 2900 | 0.86 | 0.21 | 3100 | 64 | 3.3 | 220 | 23 | 0.78 |
| $^{62}$Ni | 2100 | 0.78 | 0.18 | 3100 | 52 | 3.5 | 190 | 20 | 0.83 |
| $^{63}$Cu | 6700 | 1.40 | 0.35 | 5800 | 320 | 2.8 | 580 | 570 | 1.40 |
| $^{64}$Ni | 2400 | 0.76 | 0.26 | 1900 | 53 | 3.3 | 170 | 19 | 0.65 |
| $^{64}$Zn | 2500 | 1.60 | 0.35 | 5700 | 150 | 4.3 | 860 | 99 | 2.60 |
| $^{66}$Zn | 1700 | 1.30 | 0.30 | 6800 | 130 | 4.5 | 920 | 77 | 2.90 |
| $^{68}$Zn | 1700 | 1.10 | 0.21 | 7200 | 110 | 4.2 | 630 | 65 | 2.20 |
| $^{77}$Se | 4500 | 3.60 | 0.65 | 4800 | 490 | 3.9 | 1200 | 1200 | 2.60 |
| $^{78}$Se | 920 | 2.10 | 0.46 | 6200 | 200 | 6.4 | 1800 | 230 | 5.90 |
| $^{80}$Se | 870 | 1.70 | 0.21 | 6200 | 110 | 5.7 | 750 | 100 | 3.10 |
| $^{85}$Rb | 1400 | 11.00 | 0.89 | 6600 | 390 | 6.1 | 3600 | 700 | 7.40 |
| $^{88}$Sr | 160 | 5.40 | 0.56 | 3500 | 48 | 17.0 | 3200 | 14 | 11.00 |
| $^{89}$Y | 210 | 5.00 | 0.60 | 5400 | 100 | 20.0 | 6400 | 59 | 15.00 |
| $^{90}$Zr | 280 | 2.00 | 0.53 | 4400 | 84 | 11.0 | 2700 | 52 | 11.00 |
| $^{91}$Zr | 320 | 3.20 | 1.00 | 6100 | 220 | 15.0 | 9200 | 240 | 18.00 |
| $^{92}$Zr | 250 | 2.50 | 0.79 | 5000 | 120 | 14.0 | 5400 | 120 | 20.00 |
| $^{92}$Mo | 380 | 1.80 | 0.80 | 5700 | 160 | 12.0 | 5600 | 140 | 17.00 |
| $^{93}$Nb | 1800 | 3.10 | 1.80 | 6800 | 760 | 6.1 | 7400 | 1700 | 12.00 |
| $^{94}$Zr | 130 | 2.00 | 0.68 | 7000 | 110 | 16.0 | 7700 | 84 | 29.00 |
| $^{94}$Mo | 480 | 1.90 | 0.87 | 6700 | 240 | 11.0 | 6400 | 280 | 19.00 |
| $^{95}$Mo | 1100 | 3.00 | 2.00 | 7500 | 730 | 7.7 | 11000 | 1200 | 16.00 |
| $^{96}$Mo | 310 | 1.90 | 1.10 | 8000 | 260 | 13.0 | 11000 | 300 | 33.00 |
| $^{97}$Mo | 1500 | 3.20 | 2.10 | 8300 | 960 | 6.7 | 12000 | 1900 | 16.00 |
| $^{98}$Mo | 470 | 2.00 | 0.77 | 7800 | 240 | 11.0 | 6700 | 310 | 21.00 |
| $^{100}$Mo | 790 | 2.00 | 0.95 | 9400 | 370 | 8.4 | 7500 | 700 | 22.00 |
| $^{101}$Ru | 2000 | 2.80 | 2.10 | 7000 | 810 | 5.9 | 8600 | 1800 | 15.00 |
| $^{103}$Rh | 3900 | 3.30 | 2.80 | 7500 | 1600 | 3.9 | 8000 | 4300 | 13.00 |
| $^{105}$Pd | 2200 | 2.70 | 2.00 | 7800 | 1000 | 5.4 | 8600 | 2700 | 14.00 |
| $^{106}$Cd | 2100 | 2.90 | 1.40 | 7100 | 640 | 5.3 | 5400 | 1700 | 15.00 |
| $^{107}$Ag | 3200 | 4.10 | 2.50 | 8000 | 1600 | 4.3 | 8600 | 3600 | 12.00 |
| $^{108}$Pd | 1100 | 2.00 | 1.10 | 11000 | 570 | 7.2 | 8600 | 1500 | 25.00 |
| $^{108}$Cd | 1800 | 2.50 | 1.20 | 8400 | 680 | 5.2 | 5200 | 2100 | 16.00 |
| $^{109}$Ag | 3700 | 4.00 | 2.50 | 8300 | 1700 | 4.1 | 8300 | 4700 | 12.00 |
| $^{110}$Pd | 460 | 2.40 | 1.20 | 9900 | 390 | 12.0 | 15000 | 690 | 41.00 |
| $^{110}$Cd | 980 | 3.90 | 1.20 | 11000 | 600 | 9.3 | 11000 | 1400 | 28.00 |
| $^{111}$Cd | 3700 | 4.10 | 1.70 | 9600 | 1400 | 4.4 | 7000 | 6000 | 13.00 |
| $^{112}$Cd | 870 | 3.60 | 1.30 | 9900 | 540 | 9.2 | 11000 | 1200 | 31.00 |
| $^{113}$Cd | 3400 | 6.20 | 2.20 | 7500 | 1400 | 4.7 | 7700 | 2700 | 9.90 |
| $^{114}$Cd | 870 | 3.20 | 0.99 | 11000 | 490 | 8.7 | 9700 | 1200 | 29.00 |
| $^{115}$In | 2400 | 6.90 | 2.50 | 11000 | 1700 | 5.6 | 15000 | 3900 | 15.00 |
| $^{116}$Cd | 320 | 5.40 | 1.10 | 11000 | 380 | 20.0 | 24000 | 510 | 51.00 |
| $^{117}$Sn | 600 | 8.40 | 1.30 | 11000 | 530 | 13.0 | 19000 | 790 | 31.00 |
| $^{134}$Ba | 1600 | 15.00 | 0.74 | 8600 | 340 | 8.2 | 5300 | 570 | 16.00 |
| $^{135}$Ba | 7700 | 17.00 | 0.97 | 7700 | 910 | 4.0 | 2900 | 3300 | 5.70 |
| $^{137}$Ba | 1600 | 18.00 | 0.53 | 11000 | 340 | 9.4 | 5300 | 580 | 11.00 |
| $^{139}$La | 1700 | 6.90 | 0.45 | 15000 | 370 | 6.9 | 4700 | 780 | 11.00 |

cally the same for all nuclei. In Table I we have listed the values for $\Delta(E_m)$; the largest effect is $5.1\times10^{-3}$ for $^{116}$Cd. The values for $V_{\rm kin}$ in Table I show clearly that even at $E_m$ we are dealing with a strong kinematical *suppression,* due to the angular momentum barrier.

The remaining factors contain the *enhancement* in the proper sense. The factor $V_{\rm dyn}=(4\pi\Gamma_s^{\downarrow}/d^J)^{1/2}$ stands for the dynamical enhancement and is also listed in Table I. Following Bunakov [40] we adopt the naming resonance enhancement for the factor

$$V_{\rm res,+}=(T_L^+)^{-1/2}\approx(2\pi\Gamma_{{\rm tot},J,1}/d^{J,+})^{-1/2}$$

(similarly $V_{\rm res,-}$). The first line of Eq. (6.14) gives an estimate of the final result in terms of statistical scattering theory, i.e., the $d^{J\pi}$ and $T_c$, which are weakly dependent on *energy.* But it is useful also to separate out the terms, which are smoothly dependent on *mass number.* This is the purpose of the second form of (6.14): the first two factors contain the smooth $A$ dependence, whereas the third one may strongly vary from nucleus to nucleus. The factor $V_{\rm time}=2\Gamma_s^{\downarrow}/\Gamma_{\gamma,J,-}$ depends weakly on $A$ because both the strong spreading width and the total radiative widths do so. It clearly exhibits, that *long* lifetimes (compared to the equilibration time $\hbar/\Gamma_s^{\downarrow}$) favor the

TABLE I. (*Continued*).

| Nucleus | $E_m$ (eV) | $l$ (cm) | $V_{\rm kin}$ ($10^{-1}$) | $V_{\rm time}$ | $V_{\rm dyn}$ | $V_{\rm res}$ | $V_{\rm tot}$ | $\overline{Q_{pp}}$ ($10^{-20}$ s) | $\Delta$ ($10^{-4}$) |
|---|---|---|---|---|---|---|---|---|---|
| $^{140}$Ce | 500 | 2.90 | 0.19 | 17000 | 130 | 8.0 | 2600 | 120 | 11.00 |
| $^{143}$Nd | 6300 | 3.50 | 0.61 | 11000 | 790 | 2.5 | 1600 | 3700 | 4.40 |
| $^{144}$Nd | 2400 | 1.80 | 0.27 | 13000 | 360 | 2.8 | 980 | 870 | 4.20 |
| $^{145}$Nd | 9000 | 2.90 | 0.62 | 11000 | 1100 | 1.9 | 1300 | 7400 | 3.50 |
| $^{146}$Nd | 1700 | 2.20 | 0.28 | 20000 | 490 | 3.8 | 2100 | 1500 | 8.10 |
| $^{148}$Nd | 5100 | 3.00 | 0.35 | 13000 | 630 | 2.7 | 1300 | 2500 | 4.60 |
| $^{149}$Sm | 28000 | 3.30 | 0.65 | 12000 | 3600 | 1.3 | 1000 | 58000 | 2.00 |
| $^{150}$Sm | 4000 | 2.10 | 0.47 | 16000 | 1000 | 2.6 | 1900 | 5800 | 6.50 |
| $^{150}$Nd | 3000 | 2.50 | 0.44 | 12000 | 570 | 3.1 | 1600 | 2000 | 6.00 |
| $^{152}$Sm | 2800 | 2.60 | 0.42 | 25000 | 1000 | 3.5 | 3600 | 5500 | 11.00 |
| $^{153}$Eu | 30000 | 6.80 | 0.92 | 9800 | 4800 | 1.4 | 1300 | 62000 | 1.80 |
| $^{154}$Sm | 2900 | 3.20 | 0.57 | 11000 | 700 | 3.9 | 2400 | 2600 | 7.30 |
| $^{156}$Gd | 5800 | 3.80 | 0.69 | 10000 | 1200 | 3.2 | 2200 | 6700 | 5.80 |
| $^{159}$Tb | 9500 | 4.60 | 1.70 | 9600 | 2900 | 2.3 | 3800 | 22000 | 6.20 |
| $^{162}$Dy | 4300 | 3.50 | 0.82 | 8900 | 930 | 3.4 | 2500 | 4100 | 7.30 |
| $^{164}$Dy | 2600 | 3.10 | 0.72 | 8800 | 620 | 4.1 | 2600 | 2000 | 8.20 |
| $^{165}$Ho | 11000 | 4.30 | 1.00 | 11000 | 2500 | 2.4 | 2600 | 22000 | 4.20 |
| $^{166}$Er | 4600 | 3.40 | 0.84 | 9800 | 1200 | 3.5 | 2900 | 6300 | 7.40 |
| $^{169}$Tm | 9600 | 4.30 | 1.30 | 9300 | 2400 | 2.5 | 2900 | 17000 | 5.20 |
| $^{170}$Er | 2500 | 3.00 | 0.65 | 9400 | 670 | 4.4 | 2700 | 2200 | 7.60 |
| $^{178}$Hf | 4500 | 2.20 | 0.54 | 13000 | 950 | 3.2 | 2200 | 5000 | 7.00 |
| $^{179}$Hf | 9600 | 3.20 | 1.10 | 12000 | 2500 | 2.6 | 3400 | 22000 | 5.60 |
| $^{180}$Hf | 3000 | 2.00 | 0.44 | 13000 | 770 | 3.9 | 2300 | 3500 | 7.40 |
| $^{181}$Ta | 13000 | 2.60 | 0.64 | 13000 | 2600 | 2.5 | 2000 | 26000 | 3.10 |
| $^{182}$W | 3500 | 1.40 | 0.57 | 13000 | 920 | 3.4 | 2500 | 4600 | 7.90 |
| $^{183}$W | 6700 | 1.90 | 0.89 | 11000 | 1900 | 3.0 | 3000 | 14000 | 5.80 |
| $^{184}$W | 3700 | 1.30 | 0.49 | 12000 | 830 | 3.2 | 1900 | 4000 | 6.60 |
| $^{185}$Re | 7600 | 1.50 | 1.30 | 13000 | 3100 | 2.4 | 3900 | 32000 | 6.70 |
| $^{186}$W | 3900 | 1.50 | 0.44 | 13000 | 800 | 3.4 | 2000 | 3700 | 6.50 |
| $^{186}$Os | 6500 | 1.20 | 0.46 | 11000 | 1500 | 2.8 | 1400 | 10000 | 3.50 |
| $^{187}$Re | 8700 | 1.50 | 0.99 | 12000 | 2700 | 2.3 | 2800 | 29000 | 5.10 |
| $^{187}$Os | 14000 | 1.20 | 0.66 | 11000 | 3100 | 1.8 | 1300 | 35000 | 2.30 |
| $^{188}$Os | 6100 | 1.20 | 0.48 | 10000 | 1200 | 2.8 | 1400 | 6900 | 3.60 |
| $^{197}$Au | 6700 | 1.60 | 0.63 | 8300 | 1400 | 2.7 | 1400 | 8200 | 2.40 |
| $^{203}$Tl | 3100 | 4.40 | 0.41 | 3600 | 340 | 3.9 | 580 | 530 | 1.10 |
| $^{204}$Pb | 1000 | 3.10 | 0.33 | 5200 | 190 | 7.9 | 1300 | 150 | 2.80 |
| $^{205}$Tl | 850 | 4.70 | 0.24 | 2400 | 87 | 8.0 | 470 | 39 | 0.89 |
| $^{209}$Bi | 210 | 2.40 | 0.16 | 16000 | 94 | 13.0 | 3300 | 40 | 6.60 |
| $^{232}$Th | 1400 | 3.20 | 0.90 | 19000 | 1800 | 5.9 | 10000 | 12000 | 22.00 |
| $^{235}$U | 9600 | 2.60 | 2.40 | 16000 | 8100 | 1.8 | 6700 | 74000 | 6.60 |
| $^{236}$U | 1400 | 1.80 | 1.00 | 20000 | 1900 | 5.5 | 11000 | 14000 | 26.00 |
| $^{238}$U | 1500 | 1.70 | 0.85 | 20000 | 1600 | 5.3 | 8700 | 11000 | 22.00 |

effect; hence its naming.

The second line of (6.14) sheds light on a counterintuitive feature of our result: in Fig. 3 the curve for the odd nuclei lies *below* that of the even nuclei, even though they have the higher level densities (smaller level distances; see Table II) and should be favored by dynamical enhancement. But $\gamma$ decay is also favored by high level densities and the inverse level distance in $V_{\rm dyn}$ thus compensated by the level distance in $(T_L^-)^{-1/2} \approx (2\pi\Gamma_{\gamma,J,-}/d^{J,-})^{-1/2}$; the remaining level-distance dependence in $(T_L^+)^{-1/2} \sim (2\pi\Gamma_{\rm tot,J,+}/d^{J,+})^{-1/2}$ leads to the peculiar situation that *large* level distances may be favorable, not small ones. Note, however, that for the $s$-wave resonances $\Gamma_{\rm tot,J,+}$ is in general not dominated by the $\gamma$ channels, which weakens this counterintuitive $d^{J\pi}$ dependence.

In Table I, the determining factors of both forms are given: $V_{\rm kin}$, $V_{\rm dyn}$, $V_{\rm time}$, and $V_{\rm res,+}$ (the values for the $V_{\rm res,-}$ are similar). Both forms lead to a total enhancement factor, $V_{\rm tot} = V_{\rm kin} V_{\rm dyn} V_{\rm res,+} V_{\rm res,-}$ which is also tabulated.

Our decomposition of influence factors suggests the following strategy of finding good candidates: first, search in the favorable mass regions of the "parity forbidden strength function." Then, look at the target nuclei, where the ratio $d^{J,+}/\Gamma_{\rm tot,J,+}$ is largest (preferably among the even nuclei). Finally, choose the nucleus with the smallest $\Gamma_{\gamma,J,-}$. Note, that the nucleus $^{238}$U recently investigated experimentally is a good candidate in the sense of this strategy, whereas $^{139}$La (which showed in a single resonance the largest parity effect ever observed) appears on average as a rather poor candidate.

Many of the investigated nuclei are, for practical reasons, not suited for a target, and many of them are not really suitable for energy averaging experiments, as they exist now. One reason is that the predicted energy of the maximal effect lies outside the experimentally accessible range, and that the effect is too small within it. Another reason is that there may be only a few levels up to some keV; then, our statistical approach should be replaced by an individual resonance analysis as given in Ref. [10]. But still, our formalism gives the expected size of the parity observables (in the sense of a rms expectation value) even for these nuclei. This may be relevant for chemically or isotopically composite targets, where the effects from the different components can be estimated by taking the weighted averages of the rms expectations of different species with their abundancies or molar fractions as weights. The main reason, however, for presenting also these unsuitable candidates, is to complete the "parity forbidden strength function" of Fig. 3, i.e., the survey over mass and even/odd effects on $\Delta$.

To give an idea of the errors on our calculated results, we discuss two cases. In the first case, the complete set of input data [$D_0$, $D_1$, $S_0$, $S_1$, $S_{\gamma 0}$ (or $\Gamma_{\gamma 0}$), $S_{\gamma 1}$ (or $\Gamma_{\gamma 1}$)] is known. Typically, the largest error of one of these input data (from Refs. [51] and [52]) is smaller than 50%; the resulting error on $\Delta$ is then smaller than 30%, because all input data occur in square roots. In the second case, we have to assume values of missing data, most often for the $p$-wave radiative widths. Typically, the assumption $\Gamma_{\gamma 1} \approx \Gamma_{\gamma 0}$ may be wrong by a factor between 1 and 4, as can be seen from those examples of Table III, where both values are tabulated, not calculated. We show the effect of this uncertainty in Fig. 4 for the nucleus $^{238}$U. Additionally, we show there the error coming from the lumping of all channels in comparison to the lumping of the $\gamma$ channels alone. This error is mainly due to the $s$-wave channel; in the $p$-wave channel the total lumping approximation is a good one, as we will discuss below.

We complete the discussion with some data referring to various statements and approximations made in the text. First, the slow neutron approximation [see Eq. (3.2)]: in most cases $kR \ll 1$ (even at $E = E_m$); the largest occurring value is 0.27 for $^{153}$Eu. Second, the ratio of potential and absorption cross section: it is small (at 1 eV, $\sigma^{\rm pot}/\sigma^{{\rm abs},s} < 0.1$) or close to unity (at $E_m$) with a maximum of 2.66 for $^{235}$U. Third, the ratio of neutron and total $\gamma$-transmission coefficients for the $s$-wave resonances (alternatively the corresponding particle and radiative widths): in many cases $T_{n,0}/T_{\gamma,J,0} \gg 1$ at $E_m$ (and $\gtrsim 1$ even at 1 eV); this means that the decay of $s$-wave resonances starts to be dominated by the neutron channel at least at $E_m$.

Fourth, the same ratio for the $p$-wave resonances: in most cases $T_{n1}/T_{\gamma,J,1} \ll 1$ even at $E_m$ with a maximum value of 0.19 in $^{40}$Ca; hence, we see the predominance of radiative processes in the $p$-wave channel and the approximation (3.31) is certainly well justified. Fifth, the weak absorption approximation, see Eq. (3.27): in most cases $\sum T_c \ll 1$ with a maximum value of $\sum T_{c,J_<,+} = 0.58$ for $^{149}$Sm [values larger than 0.2 occur only for large values

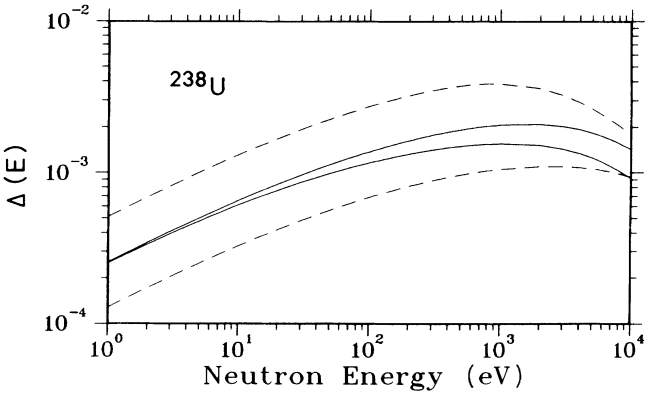


FIG. 4. Quality of the two forms of the lumping approximation and "bandwidth" of $\Delta$ due to the uncertainty in the $p$-wave radiative width. Upper solid curve, Eq. (3.29) for the interaction time integrals in (6.11), i.e., lumping of the $\gamma$ channels alone; lower solid curve, the same with Eq. (3.31) i.e., lumping of all channels. Both solid curves are calculated under the assumption $\Gamma_{\gamma 1} = \Gamma_{\gamma 0}$. Upper dashed curve, $\Gamma_{\gamma 1} = \frac{1}{4}\Gamma_{\gamma 0}$; lower dashed curve, $\Gamma_{\gamma 1} = 4\Gamma_{\gamma 0}$. Both dashed curves are calculated using Eq. (3.29) for the interaction times.

of $E_m$ ($\gtrsim 10$ keV), when the $s$-wave particle channel strongly contributes]; thus both the use of the approximation (3.28) and the neglect of external mixing (see Sec. IV C) are justified. Sixth, the average delay times for $s$-wave resonances: they are long in comparison to the time scale of a direct reaction ($10^{-21}$ s) or the mere time of passage [$\sim(1\text{ fm})/(c/10)\sim 3\times 10^{-23}$ s] of a high-energy proton by another one. The same holds for the delay times of the $p$-wave resonances, even though they are one or two orders of magnitude shorter than those of the $s$-wave resonances (which reflects the large difference in probability of exciting a $p$- or an $s$-wave resonance via the neutron channel).

## VII. SUMMARY AND OUTLOOK

The main stream of reasoning of the present work proceeded through the following steps.

A series of equations has been given that relate three different parity forbidden observables in neutron optics to the scattering matrix [Eqs. (2.5) and (3.1)], and the scattering matrix, in turn, to the underlying Hamiltonian [Eqs. (3.4)–(3.6) and (3.9)–(3.11)], which incorporates both the statistical fluctuations and parity violation.

A general result [Eqs. (3.12)–(3.14) and (3.16)–(3.23)] has been derived for the averages of the parity forbidden $S$-matrix elements (and hence, of the parity observables) depending only on average quantities [level densities, transmission coefficients (strength functions), and spreading widths].

A quite important step is achieved by a series of approximations, which subsequently simplify the general result to handy analytical expressions [Eqs. (3.26), (3.28), (3.29), and (3.31)]. It is only by virtue of these simplifications that the model can be applied to slow neutron scattering and yields numerical results for concrete nuclei.

Of more principle interest is the connection of the expected size of the parity effect on the one hand to the mean delay or Wigner-Smith time and other nuclear times, on the other hand [Eqs. (4.8)–4.10)].

A relation is given between an orthogonal invariant characterizing the size of the parity violating perturbation (a matrix norm) and the weak spreading width, which is proposed to be the physical parameter [Eqs. (4.4) and (4.5)].

A practically quite important question is to which extend finite energy resolution affects the observable energy averaged effects. The energy spread of the experimental setup acts as a virtual broadening of the observable linewidth, which, in turn, is a decisive factor for the magnitude of the observables. This qualitative understanding is made quantitative for various physical situations.

The main achievement of the present work are numerical results for 99 nuclei with mass numbers from $A=32$ to $A=238$ (see Figs. 2 and 3 and Table I). Typical rms values of the parity observables range from $10^{-4}$ to $5\times 10^{-3}$ (at the energy, where the maximum occurs), thus largely profiting from the enhancement mechanisms explained in Sec. II B. The general behavior, i.e., mass number and even/odd effects, is explained in terms of the average input parameters (level densities and optical model strength functions). It is mainly in order to make this survey as general as possible that we studied so many nuclei (note that a considerable number out of them is, for various reasons, not suited for experiment). In this sense, the present results serve as an illustration of the predictive power of the approach developed in Ref. [11].

Concerning extensions of the above-mentioned results, there are strong reasons [57] to generalize the *overall* energy averaging procedure (where all energy points are treated equivalently, i.e., in an unbiased way) to *biased* averaging, where special points on the energy axis are selected or rejected. A first reason is the "black resonance problem," i.e., the vanishing of transmitted intensity and hence the loss of counting statistics close to strongly absorptive $s$-wave resonances, which, consequently, should be discarded from consideration. An even more important reason is the following one: qualitatively, the enhancement of symmetry violations is due to the presence of long-lived and closely spaced resonances, hence large effects will somehow be "concentrated" in their neighborhood. Biasing, i.e., selecting these resonance neighborhoods before averaging, brings up an additional enhancement, which turns out to be [58–61] roughly another resonance enhancement factor, i.e., the square root of the distance to width ratio of the levels, and which lies between 1 and 10 (see Sec. IV C). This form of biasing is especially important for $T$-violation studies, where an upper bound is expected rather than a definite nonzero effect (as one has for $P$ violation).

An even more important extension may be necessary if the sign correlations found in a recent experiment [62] with $^{232}$Th turn out to be a general phenomenon. Then, in addition to the fluctuating part of the parity forbidden scattering amplitude $\Delta f$, one has a "direct" or "correlated" part with nonvanishing average $\overline{\Delta f}\neq 0$. Various mechanisms for this have been proposed [63], but a clear-cut answer is, for the time being, not available. It is, however, clear, that a fluctuating part must be present in any case, because the experimental data [12,62] show strong fluctuations around the average value. Under these circumstances, the present work is a valid model for the fluctuating part. Its numerical predictions may be useful for planning future experiments and interpreting their results. Especially, if a separation in "direct" and "fluctuating" contributions to parity-forbidden observables really turns out to be necessary in general, it is important to have a reliable model for both of them.

Two final statements seem to be of general interest: It is a noteworthy phenomenon that the effects of such a weak perturbation as, for instance, parity violation (characterized by an energy $\Gamma_w^{\downarrow}\approx 10^{-7}$ eV) do not only survive upon averaging over such a strongly fluctuating system as the compound nucleus (characterized by a temperature $\sim 1$ MeV), but even get enhanced. Furthermore, it is even possible to predict the rms expectation values of such effects by means of statistical scattering theory.

## ACKNOWLEDGMENTS

A.M. gratefully acknowledges financial support from the Studienstiftung des Deutschen Volkes, the Freundeskreis der Universität Heidelberg, and the Deutsche Forschungsgemeinschaft. He furthermore wishes to thank C. Lewenkopf and F. M. Dittes for helpful discussions and M. Uhl for valuable comments on the neutron data.


## APPENDIX A: PROOF OF THE LUMPING APPROXIMATION (3.26)

First we split the product function in the $N_l$ channels to be lumped into three product functions

$$\prod_l^{N_l} \frac{1-T_l\lambda}{\sqrt{1+T_l\lambda_1}\sqrt{1+T_l\lambda_2}} = \prod_l^{N_l}(1+T_l\lambda_1)^{-1/2}\prod_l^{N_l}(1+T_l\lambda_2)^{-1/2}\prod_l^{N_l}(1-T_l\lambda)\ . \tag{A1}$$

Introducing the average transmission coefficient and the deviations from it in the lumped subset of channels

$$\langle T_l\rangle = \frac{1}{N_l}\sum_l^{N_l} T_l, \quad \Delta T_l = T_l - \langle T_l\rangle \tag{A2}$$

we can rewrite each of the factors in (A1) in the following form (for $\lambda_2$, $\lambda$ analogously):

$$\prod_l^{N_l}(1+T_l\lambda_1)^{-1/2} = (1+\langle T_l\rangle\lambda_1)^{-N_l/2}\prod_l^{N_l}\left[1+\frac{\Delta T_l\lambda_1}{1+\langle T_l\rangle\lambda_1}\right]^{-1/2}\ . \tag{A3}$$

Under the assumption that $N_l \gg 1$, the first factor on the right-hand side becomes

$$(1+\langle T_l\rangle\lambda_1)^{-N_l/2} = \left[1+\frac{\lambda_1\sum T_l}{N_l}\right]^{-N_l/2} \approx \exp\left[-\lambda_1\sum T_l/2\right]\ . \tag{A4}$$

This is an exponential cutoff factor, essentially vanishing for $\lambda_1 \geq 2/\sum T_l$. Now it remains to show that the second factor on the right-hand side in (A3) becomes unity under the assumption, that $N_l \gg 1$ and that $\langle(\Delta T)^2\rangle$ exists: then, $T_l/\sum T_l \sim 1/N_l \ll 1$. Consider the logarithm

$$\begin{aligned}
\ln\prod_l^{N_l}\left[1+\frac{\Delta T_l\lambda_1}{1+\langle T_l\rangle\lambda_1}\right]^{-1/2} &= -\frac{1}{2}\sum_l^{N_l}\ln\left[1+\frac{\Delta T_l\lambda_1}{1+\langle T_l\rangle\lambda_1}\right] \\
&\approx -\frac{1}{2}\sum_l^{N_l}\left[\frac{\Delta T_l\lambda_1}{1+\langle T_l\rangle\lambda_1} - \frac{1}{2}\left[\frac{\Delta T_l\lambda_1}{1+\langle T_l\rangle\lambda_1}\right]^2\right] \\
&\leq \left[\frac{1}{N_l\langle T\rangle}\right]^2\sum_l^{N_l}(\Delta T_l)^2 \\
&= N_l^{-1}\frac{\langle T^2\rangle - \langle T\rangle^2}{\langle T\rangle^2}\ .
\end{aligned} \tag{A5}$$

In the second line, the linear term vanishes exactly due to the very definition of the $\Delta T_l$; the various factors in the quadratic term are then replaced by the estimates

$$\lambda_1 \lesssim 2/\sum T_l, \quad 1+\langle T_l\rangle\lambda_1 \geq 1\ . \tag{A6}$$

In the third line, we recognize the second moment of the $T_l$'s, which gives the final result. The second factor in (A3) thus turns out to be $\sim e^{N_l^{-1}}$, which differs negligibly from unity, if $N_l$ is large enough and the ratio of the moments exists.

## APPENDIX B: PROOF OF THE INTERACTION TIME EXPRESSION (4.8)

First we have to prove another property of our model, ensuing from ergodicity. The ensemble average $\overline{f(E)}$ of some energy dependent quantity $f(E)$ is equivalent to the energy average of $f(E)$. The latter, in turn, is by definition independent from $E$. Hence

$$\frac{\partial}{\partial E}\overline{f(E)} = 0\ . \tag{B1}$$

Together with the property (3.8) we find

$$\overline{G^2} = \frac{\partial}{\partial E}\overline{G} = 0\ , \tag{B2}$$

analogously for higher powers of $G$ and $G^*$. [Note that (B2) does not hold for mixed powers of the form $G^m(G^*)^n$ with $m,n \neq 1$.]

Now starting from Eq. (3.15) we write

$$\begin{aligned}\overline{Q_{p\bar{p}}} &= 2\pi\hbar\overline{(V^T G^* G V)_{p\bar{p}}} \\ &= 2\pi\hbar\overline{(V^T(G-G^*)G^* V)_{p\bar{p}}} \\ &= -(2\pi)^2 i\hbar\overline{(V^T(GVV^TG^*)G^* V)_{p\bar{p}}} \\ &= (2\pi)^2 i\hbar\overline{\left[(V^T G V)\frac{\partial}{\partial E}(V^T G^* V)\right]_{p\bar{p}}} \\ &= i\hbar[1-2\pi i(V^T G V)]\frac{\partial}{\partial E}[1+2\pi i(V^T G^* V)]_{p\bar{p}} \\ &= i\hbar\overline{\left[S\frac{\partial}{\partial E}S^*\right]_{p\bar{p}}} . \end{aligned} \tag{B3}$$

Here, we have subsequently used stationarity in the form (B2) (second line); unitarity in the form (3.7) (third line); the analytic property (3.8) (fourth line); again stationarity in the form (B2) (fifth line); the definition of $S$, see Eq. (3.4) (last line). Starting from this result, Eq. (3.18) can be derived using the final equation of Ref. [11] and ergodicity.

## APPENDIX C: PROOF OF THE FINITE RESOLUTION RECIPES (5.5) AND (5.12)

We write the energy-dependent parts of (5.2) explicitly:

$$\overline{L_p(\epsilon)} = \frac{d^+}{h}\frac{1}{8}\int d\lambda_1 \int d\lambda_2 \int d\lambda \mu(\Lambda)\prod\nolimits_{\vec{T}}(\Lambda) e^{-i\pi(\epsilon/d)(\lambda_1+\lambda_2+2\lambda)} q_p(\Lambda) . \tag{C1}$$

The whole expression is of the form (3.18), but with an additional exponential factor containing the whole dependence on $E_1$, $E_2$ in form of the difference $\epsilon = E_2 - E_1$. Inserting (C1) into (5.3) leads to expressions of the following form [with the abbreviation $\pi(\lambda_1+\lambda_2+2\lambda)/d = \omega$]:

$$\begin{aligned}&\int_{-\infty}^{\infty} dE_2' \int_{-\infty}^{\infty} dE_1' e^{-i(E_2'-E_1')\omega} r(E_2-E_2')r(E_1-E_1') \\ &= \int_{-\infty}^{\infty} d\epsilon' \int_{-\infty}^{\infty} dE_1' e^{-i\epsilon'\omega} r[E_2-(\epsilon'+E_1')]r(E_1-E_1') \\ &= \int_{-\infty}^{\infty} d\epsilon' \int_{-\infty}^{\infty} dE_1' e^{-i\epsilon'\omega} r(\epsilon-\epsilon'-E_1')r(-E_1') \\ &= \int_{-\infty}^{\infty} d\epsilon' e^{-i\epsilon'\omega} r * r(\epsilon-\epsilon') \\ &= e^{-i\epsilon\omega}\int_{-\infty}^{\infty} d\epsilon'' e^{i\epsilon''\omega} r * r(\epsilon'') \\ &= e^{-i\epsilon\omega}\tilde{r}^2(\omega) . \end{aligned} \tag{C2}$$

The second line follows from the substitution $E_1' - E_2' = \epsilon'$; the third follows from the shift $E_1' \to E_1' - E_1$. Assuming $r(E) = r(-E)$, i.e., symmetry of the resolution function, and the definition $r * r(\epsilon) = \int r(\epsilon')r(\epsilon-\epsilon')d\epsilon'$ for the convolution, yields the fourth line. Another substitution $\epsilon - \epsilon' = \epsilon''$ gives the fifth; the folding theorem of Fourier transformations ((4.4.2.1.) of Ref. [64]) gives the last line.

Interpreting Eq. (C2), we rediscover the original Fourier factor, multiplied by $\tilde{r}^2(\omega)$ (the square of the Fourier transform of the autocorrelation of $r$). Inserting (C2) into (5.3) we see that the modification due to the final resolution means nothing but multiplying the whole integrand by this factor $\tilde{r}^2(\omega)$. For convenience, we group it together with $\prod_{\vec{T}}(\Lambda)$ and obtain Eq. (5.5).

In the case of correlated measurements of $L_{pp}L_{mm}$ we obtain expressions of the form of Eq. (5.11). Note that both $\overline{L_{pp}(\epsilon)}$ and $\overline{L_{mm}(\epsilon)}$ are threefold integrations with different integration arguments and, hence, different Fourier factors $e^{-i\epsilon'\omega^+}$, $\omega^+ = \pi(\lambda_1+\lambda_2+2\lambda)/d^+$ and $e^{-i\epsilon'\omega^-}$, $\omega = \pi(\lambda_1'+\lambda_2'+2\lambda')/d^-$, respectively. (In the case of isolated resonances and lumped channels, $\omega^+ = \pi x/d^+$, $\omega^- = \pi x/d^-$.) The energy dependent part of Eq. (5.11) reads as follows:

$$\begin{aligned}&\int_{-\infty}^{\infty} dE_2' \int_{-\infty}^{\infty} dE_1' e^{-i(E_2'-E_1')\omega^-} e^{-i(E_2'-E_1')\omega^+} r(E_1-E_1')r(E_2-E_2') \\ &\qquad = \int_{-\infty}^{\infty} dE_2' \int_{-\infty}^{\infty} dE_1' e^{-i(E_2'-E_1')(\omega^-+\omega^+)} r(E_1-E_1')r(E_2-E_2') , \end{aligned} \tag{C3}$$

i.e., it is exactly of the starting form of Eq. (C2) with the replacement $\omega \to \omega^- + \omega^+$, occurring in the argument of $\tilde{r}^2$. If we want that the two threefold integrations depending on $\omega^-$ and $\omega^+$ remain independent of each other, we have to require

$$\tilde{r}(\omega^-+\omega^+) = \tilde{r}(\omega^-)\tilde{r}(\omega^+) , \tag{C4}$$

which is the functional equation of the exponential. But the only resolution function whose Fourier transform is an exponential is a Lorentzian. In this case, $\tilde{r}(\omega^-)$ and $\tilde{r}(\omega^+)$ can be grouped with the other functions depending on $\lambda_1$, $\lambda_2$,

$\lambda$ and $\lambda_1'$, $\lambda_2'$, $\lambda'$, respectively, leading back to products of expressions like (5.3). We have thus proven (5.12).

In the general case, however, the factorization (C4) does not hold and we show the use of $r(\omega^-+\omega^+)$ for the case of isolated and lumped resonances, i.e., where [34]

$$\overline{L_p(\epsilon)}=\frac{T_p}{2}\int_0^\infty dx\, e^{-T_L^+x/2}e^{-i\pi(\epsilon/d^+)x} \tag{C5}$$

with $T_L^+$ as in Eq. (3.30). Inserting this and (C2) with $r(\omega^-+\omega^+)$ into (5.11) gives

$$\begin{aligned}\overline{L_pL_m}^{E\pm\Delta E}&=\frac{T_pT_m}{4}\int_0^\infty\int_0^\infty dx\,dx' e^{-T_L^+x/2}e^{-T_L^-x/2}\tilde{r}\left[\pi\frac{x}{d^+}+\pi\frac{x'}{d^-}\right]\\&=\frac{T_pT_m}{T_L^+T_L^-}\int_0^\infty\int_0^\infty dy\,dy' e^{-(y+y')}\tilde{r}^2\left[y\frac{T_R^+}{T_L^+}+y'\frac{T_R^-}{T_L^-}\right]\end{aligned} \tag{C6}$$

upon introduction of (5.8) and a suitable change of arguments. This form makes the entanglement of arguments by a simultaneous measurement [mentioned below Eq. (5.11)] explicit. For Gaussian resolution with spread $\Delta E$ we have $\tilde{r}^2(\omega)=e^{-(\Delta E\omega)^2}$ [cf. Eq. (5.7)] which leads from (C6) to (5.13) by use of standard tables of mathematical physics [36]. Finally, with $h(x)=e^{x^2}\mathrm{erfc}(x)$ we may rewrite the limit $\Gamma_L^+\to\Gamma_L^-$ or, equivalently, $R_+\to R_-=R$ as

$$\begin{aligned}\lim_{R_+\to R_-}\overline{L_pL_m}^{E\pm\Delta E}&=\lim_{R_+\to R_-}\frac{T_pT_m}{T_L^+T_L^-}\sqrt{\pi}R^+R^-\\&\quad\times\frac{h(R^-)-h(R^+)}{R^+-R^-}\\&=-\frac{T_pT_m}{T_L^2}\sqrt{\pi}R^2h'(R)\ ,\end{aligned} \tag{C7}$$

which leads to (5.14) by use of Eq. (7.2.8) of Ref. [36] for $h'$.

## APPENDIX D: EXTRACTION OF INPUT DATA

We start with the extraction of level distances $d^{J\pi}$ of resonances with given $J^\pi$ (which is needed in our theory) from the level distances $D_l$ of $l$-wave resonances, (which are found in tables [51,54,55]). The compound nucleus level densities are quite well approximated by a product of a spin- and an energy-dependent part:

$$\rho(E,J)=\mathcal{N}(2J+1)e^{-(J+1/2)^2/2\sigma^2}\rho_E=\mathcal{N}\rho_J\rho_E\ , \tag{D1}$$

where $\mathcal{N}$ is a normalization constant and $\rho_E$ the energy-dependent part—neither of which is specified here, because they drop out of the final results.

Summing over the different $J'$ allowed for one value of $l$, ($|I-l-\frac{1}{2}|\le J'\le I+l+\frac{1}{2}$), the level densities add up to

$$\rho_l=\sum_{J'}\rho(E,J')\ . \tag{D2}$$

The level distances are the reciprocal level densities:

$$d^{J\pi}=\frac{1}{\rho(E,J)} \tag{D3}$$

and

$$\begin{aligned}D_l=\frac{1}{\rho_l}&=\left[\sum_{J'}\rho(E,J')\right]^{-1}\\&=\left[\sum(d^{J'\pi})^{-1}\right]^{-1},\end{aligned} \tag{D4}$$

i.e., the level distance of the mixed sequence (measured) is the harmonic mean of the level distances of the pure sequences (needed). Using (D1) in (D4) gives

$$\frac{d^{J\pi}}{D_l}=\frac{(\mathcal{N}\rho_E\rho_J)^{-1}}{(\mathcal{N}\rho_E\sum_{J'}\rho_{J'})^{-1}}=\sum_{J'}\frac{\rho_{J'}}{\rho_J}\ . \tag{D5}$$

As claimed above, only the spin dependence matters; using its explicit form given in (D1) we obtain

$$d^{J\pi}=D_l\sum_{J'=|I-l-1/2|}^{I+l+1/2}\frac{2J'+1}{2J+1}e^{-(J'-J)(J'+J+1)/2\sigma^2}\ . \tag{D6}$$

This is identical with Eq. (6.7). Through very similar considerations, we also obtain

$$D_1=D_0\sum_{|I-1/2|}^{I+1/2}\rho_J\Big/\sum_{|I-3/2|}^{I+3/2}\rho_{J'} \tag{D7}$$

if only $D_0$ is given and

$$D_l=D\left[\sum_{|I-1/2|}^{I+1/2}\rho_J+\sum_{|I-3/2|}^{I+3/2}\rho_{J'}\right]\Big/\sum_{|I-l-1/2|}^{I+l+1/2}\rho_{J''} \tag{D8}$$

if neither $D_0$ nor $D_1$ is given, but only $D$. Note that contrary to (D6), the latter equations lead to $D^{J\pi}$ which are *independent* of $\pi$, because we apply the $\pi$-independent form (D1) to one input datum only [and not two, as in the case of (D6)].

Next we consider the sum of $\gamma$-transmission coefficients. The related strength functions are defined by

$$S_{\gamma l}=\frac{\langle\Gamma_{\gamma l}\rangle}{D_l}\ , \tag{D9}$$

where $\Gamma_{\gamma l}$ is the total radiation width. We write *all* $l$-wave resonances in terms of averages over resonances with *given* $J$:

$$\langle\Gamma_{\gamma l}\rangle=\sum_J\omega_J\langle\Gamma_{\gamma lJ}\rangle\ , \tag{D10}$$

TABLE II. Level spacings in eV; $D$, $D_0$, $D_1$ are as in Mughabghab *et al.* [49,50], the $d^{J\pi}$ refer to pure spacings as explained in Appendix D (with $J_< = I - \frac{1}{2}$ and $J_> = I + \frac{1}{2}$). There are three classes of data: without superscript if both $D_0$ and $D_1$ are given [Eq. (D6)]; with superscript $a$ if $D_0$ is given and $D_1$ calculated from it [Eq. (D7)]; with superscript $b$ if both $D_0$ and $D_1$ are calculated from $D$ [Eq. (D8)].

| Nucleus | $D$ | $D_0$ | $D_1$ | $d^{J_<+}$ | $d^{J_<-}$ | $d^{J_>+}$ | $d^{J_>-}$ |
|---|---|---|---|---|---|---|---|
| $^{32}$S | 17000 | 62000$^b$ | 23000$^b$ | | | 62000 | 62000 |
| $^{40}$Ca | | 45000 | 17000$^a$ | | | 45000 | 45000 |
| $^{43}$Ca | 1500 | 4300$^b$ | 2300$^b$ | 7800 | 7800 | 9600 | 9600 |
| $^{50}$Cr | | 15000 | 4100 | | | 15000 | 11000 |
| $^{52}$Cr | | 42000 | 14000 | | | 42000 | 38000 |
| $^{54}$Fe | | 13000 | 4400 | | | 13000 | 12000 |
| $^{55}$Mn | | 2700 | 1300 | 5500 | 4700 | 5300 | 4600 |
| $^{56}$Fe | | 17000 | 4000 | | | 17000 | 11000 |
| $^{57}$Fe | | 6000 | 2200 | 22000 | 16000 | 8200 | 6000 |
| $^{58}$Fe | | 35000 | 8300 | | | 35000 | 23000 |
| $^{58}$Ni | | 13700 | 4100 | | | 14000 | 11000 |
| $^{60}$Ni | | 16000 | 4300 | | | 16000 | 12000 |
| $^{62}$Ni | | 19100 | 8000 | | | 19000 | 22000 |
| $^{63}$Cu | | 320 | 180$^a$ | 760 | 760 | 550 | 550 |
| $^{64}$Ni | | 19900 | 7300$^a$ | | | 20000 | 20000 |
| $^{64}$Zn | | 3440 | 680 | | | 3400 | 1900 |
| $^{66}$Zn | | 4700 | 840 | | | 4700 | 2300 |
| $^{68}$Zn | | 5770 | 1290 | | | 5800 | 3500 |
| $^{77}$Se | | 146 | 100 | 550 | 760 | 200 | 280 |
| $^{78}$Se | | 1390 | 515 | | | 1400 | 1400 |
| $^{80}$Se | | 3500 | 2200 | | | 3500 | 6100 |
| $^{85}$Rb | | 200 | 100 | 420 | 380 | 380 | 350 |
| $^{88}$Sr | | 25000 | 8700 | | | 25000 | 24000 |
| $^{89}$Y | | 4000 | 1800 | 15000 | 14000 | 5400 | 5000 |
| $^{90}$Zr | | 6400 | 3500 | | | 6400 | 9700 |
| $^{91}$Zr | | 570 | 340 | 1200 | 1300 | 1100 | 1200 |
| $^{92}$Zr | | 2600 | 1900 | | | 2600 | 5300 |
| $^{92}$Mo | | 2100 | 750$^a$ | | | 2100 | 2100 |
| $^{93}$Nb | | 44 | 23$^a$ | 81 | 81 | 96 | 96 |
| $^{94}$Zr | | 3600 | 1800 | | | 3600 | 5000 |
| $^{94}$Mo | | 975 | 350$^a$ | | | 980 | 980 |
| $^{95}$Mo | | 55 | 30$^a$ | 120 | 120 | 100 | 100 |
| $^{96}$Mo | | 850 | 300$^a$ | | | 850 | 850 |
| $^{97}$Mo | | 32 | 17$^a$ | 68 | 68 | 60 | 60 |
| $^{98}$Mo | | 970 | 350$^a$ | | | 970 | 970 |
| $^{100}$Mo | | 400 | 140$^a$ | | | 400 | 400 |
| $^{101}$Ru | 16 | 45$^b$ | 25$^b$ | 97 | 97 | 86 | 86 |
| $^{103}$Rh | | 16 | 7.70$^a$ | 61 | 61 | 22 | 22 |
| $^{105}$Pd | 10 | 28$^b$ | 15$^b$ | 61 | 61 | 53 | 53 |
| $^{106}$Cd | | 135 | 48$^a$ | | | 140 | 140 |
| $^{107}$Ag | | 16 | 7.70$^a$ | 61 | 61 | 22 | 22 |
| $^{108}$Pd | 45 | 170$^b$ | 61$^b$ | | | 170 | 170 |
| $^{108}$Cd | | 120 | 43$^a$ | | | 120 | 120 |
| $^{109}$Ag | | 14 | 6.80$^a$ | 53 | 53 | 19 | 19 |
| $^{110}$Pd | 95 | 360$^b$ | 130$^b$ | | | 360 | 360 |
| $^{110}$Cd | | 155 | 55$^a$ | | | 160 | 160 |
| $^{111}$Cd | | 20 | 9.60$^a$ | 76 | 76 | 27 | 27 |
| $^{112}$Cd | | 190 | 68$^a$ | | | 190 | 190 |
| $^{113}$Cd | | 21 | 10$^a$ | 81 | 81 | 29 | 29 |
| $^{114}$Cd | | 235 | 84$^a$ | | | 240 | 240 |
| $^{115}$In | | 9.40 | 4.90$^a$ | 18 | 18 | 20 | 20 |
| $^{116}$Cd | | 390 | 140$^a$ | | | 390 | 390 |
| $^{117}$Sn | 48 | 150$^b$ | 71$^b$ | 560 | 560 | 200 | 200 |
| $^{134}$Ba | 127 | 490$^b$ | 170$^b$ | | | 490 | 490 |
| $^{135}$Ba | | 40 | 22$^a$ | 99 | 99 | 67 | 67 |
| $^{137}$Ba | | 290 | 160$^a$ | 720 | 720 | 490 | 490 |

where each $J$ is weighted with the relative frequency

$$\omega_J = \frac{D_l}{D^{J\pi}} \ . \tag{D11}$$

Now the $J$ dependence of $\langle \Gamma_{\gamma lJ} \rangle$ is weak, which for instance can be seen in the following model result ([51], Eq. (88)):

$$\langle \Gamma_{\gamma lJ} \rangle \propto d(E,J^\pi) \int_0^E \frac{E'^3}{d(E'-E,J^\pi)} dE \ , \tag{D12}$$

where the spin dependence cancels. Formally (D10) becomes

$$\langle \Gamma_{\gamma l} \rangle = \langle \Gamma_{\gamma lJ} \rangle \sum \omega_J = \langle \Gamma_{\gamma lJ} \rangle 1 \ . \tag{D13}$$

Thus, if the widths are tabulated, we can combine them directly with the result (D6) for the level densities to get

$$T_{\gamma J\pi} = 2\pi \frac{\langle \Gamma_{\gamma lJ} \rangle}{d^{J\pi}} \ . \tag{D14}$$

And if the strength functions are tabulated, inserting (D13) and (D6) into (D9) yields

TABLE II. (*Continued*).

| Nucleus | $D$ | $D_0$ | $D_1$ | $d^{J<+}$ | $d^{J<-}$ | $d^{J>+}$ | $d^{J>-}$ |
|---|---|---|---|---|---|---|---|
| $^{139}$La | | 208 | 110[a] | 420 | 420 | 410 | 410 |
| $^{140}$Ce | | 3200 | 1100[a] | | | 3200 | 3200 |
| $^{143}$Nd | | 45 | 24[a] | 91 | 91 | 89 | 89 |
| $^{144}$Nd | | 430 | 150[a] | | | 430 | 430 |
| $^{145}$Nd | | 22 | 12[a] | 44 | 44 | 44 | 44 |
| $^{146}$Nd | | 235 | 83[a] | | | 240 | 240 |
| $^{148}$Nd | | 140 | 49[a] | | | 140 | 140 |
| $^{149}$Sm | | 2.20 | 1.20[a] | 4.50 | 4.50 | 4.40 | 4.40 |
| $^{150}$Sm | | 55 | 19[a] | | | 55 | 55 |
| $^{150}$Nd | | 174 | 61[a] | | | 170 | 170 |
| $^{152}$Sm | | 51 | 18[a] | | | 52 | 52 |
| $^{153}$Eu | | 1.30 | 0.70[a] | 2.80 | 2.80 | 2.40 | 2.40 |
| $^{154}$Sm | | 115 | 41[a] | | | 120 | 120 |
| $^{156}$Gd | | 37 | 13[a] | | | 38 | 38 |
| $^{159}$Tb | | 3.90 | 2.10[a] | 9.70 | 9.70 | 6.50 | 6.50 |
| $^{162}$Dy | | 64 | 23[a] | | | 65 | 65 |
| $^{164}$Dy | | 147 | 52[a] | | | 150 | 150 |
| $^{165}$Ho | | 4.60 | 2.40[a] | 9.40 | 9.40 | 9.00 | 9.00 |
| $^{166}$Er | | 38 | 13[a] | | | 38 | 38 |
| $^{169}$Tm | | 7.30 | 3.50[a] | 28 | 28 | 9.90 | 9.90 |
| $^{170}$Er | | 125 | 44[a] | | | 130 | 120 |
| $^{178}$Hf | | 62 | 22[a] | | | 62 | 62 |
| $^{179}$Hf | | 4.40 | 2.30[a] | 8.60 | 8.60 | 9.10 | 9.10 |
| $^{180}$Hf | | 94 | 33[a] | | | 94 | 94 |
| $^{181}$Ta | | 4.17 | 2.20[a] | 8.50 | 8.50 | 8.10 | 8.10 |
| $^{182}$W | | 66 | 23[a] | | | 66 | 66 |
| $^{183}$W | | 12 | 5.70[a] | 46 | 46 | 16 | 16 |
| $^{184}$W | | 81 | 28[a] | | | 81 | 81 |
| $^{185}$Re | | 3.10 | 1.70[a] | 6.80 | 6.80 | 5.70 | 5.70 |
| $^{186}$W | | 87 | 30[a] | | | 87 | 87 |
| $^{186}$Os | | 26 | 9.10[a] | | | 26 | 26 |
| $^{187}$Re | | 4.10 | 2.20[a] | 9.00 | 9.00 | 7.50 | 7.50 |
| $^{187}$Os | | 4.40 | 2.10[a] | 17 | 17 | 5.90 | 5.90 |
| $^{188}$Os | | 40 | 14[a] | | | 40 | 40 |
| $^{197}$Au | | 16 | 8.80[a] | 41 | 41 | 27 | 27 |
| $^{203}$Tl | | 360 | 170[a] | 1400 | 1400 | 490 | 490 |
| $^{204}$Pb | | 1520 | 530[a] | | | 1500 | 1500 |
| $^{205}$Tl | | 5500 | 2600[a] | 21000 | 21000 | 7400 | 7400 |
| $^{209}$Bi | | 4500 | 1100 | 8800 | 4100 | 9200 | 4300 |
| $^{232}$Th | | 16 | 5.90[a] | | | 17 | 17 |
| $^{235}$U | | 0.44 | 0.23[a] | 0.91 | 0.91 | 0.85 | 0.85 |
| $^{236}$U | | 14 | 5.10[a] | | | 15 | 15 |
| $^{238}$U | | 20 | 7.20 | | | 21 | 21 |

TABLE III. Radiation widths and strength functions [Eq. (D9)] for $s$-wave ($\Gamma_{\gamma 0}$,$S_{\gamma 0}$) and $p$-wave ($\Gamma_{\gamma 1}$,$S_{\gamma 1}$) resonances as in Mughabghab *et al.* [49,50] and corresponding transmission coefficients [Eq. (D14)]. There are three classes of data: without superscript if the strength function is given; with superscript *a* if the strength function is calculated from the corresponding width; with superscript *b* if, for the $p$ resonances, neither $S_{\gamma 1}$ nor $\Gamma_{\gamma 1}$ is given, but the latter set to $\Gamma_{\gamma 1}=\Gamma_{\gamma 0}$.

| Nucleus | $S_{\gamma 0}$ ($10^{-4}$) | $\Gamma_{\gamma 0}$ (meV) | $S_{\gamma 1}$ ($10^{-4}$) | $\Gamma_{\gamma 0}$ (meV) | $T_{\gamma,J_<,+}$ | $T_{\gamma,J_<,-}$ | $T_{\gamma,J_>,+}$ | $T_{\gamma,J_>,-}$ |
|---|---|---|---|---|---|---|---|---|
| | | | | | ($10^{-3}$) | | | |
| $^{32}$S | 0.31[a] | 1900 | 0.81[a] | 1900 | | | 0.19 | 0.19 |
| $^{40}$Ca | 0.33 | 1500 | 0.21[a] | 360 | | | 0.21 | 0.05 |
| $^{43}$Ca | 1.70[a] | 750 | 3.30[b] | 750 | 0.61 | 0.61 | 0.49 | 0.49 |
| $^{50}$Cr | 1.00 | 1500 | 0.90 | 370 | | | 0.63 | 0.21 |
| $^{52}$Cr | 0.44 | 1900 | 0.22 | 310 | | | 0.28 | 0.05 |
| $^{54}$Fe | 1.40 | 1800 | 0.90 | 400 | | | 0.88 | 0.21 |
| $^{55}$Mn | 2.80[a] | 750 | 3.10[a] | 400 | 0.86 | 0.53 | 0.89 | 0.55 |
| $^{56}$Fe | 0.50 | 900 | 0.75 | 300 | | | 0.31 | 0.17 |
| $^{57}$Fe | 3.20 | 1900 | 3.40 | 750 | 0.54 | 0.29 | 1.50 | 0.78 |
| $^{58}$Fe | 0.90 | 3000 | 0.50 | 410 | | | 0.57 | 0.12 |
| $^{58}$Ni | 1.90 | 2600 | 6.30[b] | 2600 | | | 1.20 | 1.50 |
| $^{60}$Ni | 1.10 | 1700 | 2.10 | 900 | | | 0.69 | 0.48 |
| $^{62}$Ni | 0.50 | 910 | 1.10[b] | 910 | | | 0.31 | 0.26 |
| $^{63}$Cu | 16 | 500 | 13[a] | 260 | 4.20 | 2.10 | 5.80 | 3.00 |
| $^{64}$Ni | 1.10 | 2400 | 3.30[b] | 2400 | | | 0.69 | 0.76 |
| $^{64}$Zn | 2.10[a] | 726 | 4.00[a] | 270 | | | 1.30 | 0.92 |
| $^{66}$Zn | 0.85[a] | 400 | 2.30[a] | 190 | | | 0.53 | 0.52 |
| $^{68}$Zn | 0.55[a] | 320 | 1.30[a] | 170 | | | 0.35 | 0.30 |
| $^{77}$Se | 27[a] | 390 | 39[b] | 390 | 4.50 | 3.20 | 12 | 8.80 |
| $^{78}$Se | 1.70[a] | 230 | 4.50[b] | 230 | | | 1.00 | 1.00 |
| $^{80}$Se | 0.66[a] | 230 | 1.00[b] | 230 | | | 0.41 | 0.24 |
| $^{85}$Rb | 10 | 200 | 21[b] | 200 | 3.00 | 3.40 | 3.30 | 3.70 |
| $^{88}$Sr | 0.09[a] | 225 | 0.83[a] | 720 | | | 0.06 | 0.19 |
| $^{89}$Y | 0.25 | 100 | 1.70 | 310 | 0.04 | 0.14 | 0.12 | 0.38 |
| $^{90}$Zr | 0.40 | 260 | 1.30 | 460 | | | 0.25 | 0.29 |
| $^{91}$Zr | 2.00 | 110 | 7.00 | 240 | 0.59 | 1.10 | 0.66 | 1.30 |
| $^{92}$Zr | 0.50 | 130 | 1.90 | 360 | | | 0.31 | 0.43 |
| $^{92}$Mo | 0.90[a] | 190 | 3.60[a] | 280 | | | 0.57 | 0.82 |
| $^{93}$Nb | 38[a] | 165 | 83[a] | 190 | 13 | 15 | 11 | 12 |
| $^{94}$Zr | 0.40 | 140 | 1.00 | 180 | | | 0.25 | 0.23 |
| $^{94}$Mo | 1.40[a] | 140 | 5.70[a] | 200 | | | 0.90 | 1.30 |
| $^{95}$Mo | 29[a] | 160 | 53[b] | 160 | 8.60 | 8.60 | 9.70 | 9.70 |
| $^{96}$Mo | 1.30[a] | 110 | 4.60[a] | 140 | | | 0.81 | 1.00 |
| $^{97}$Mo | 41[a] | 130 | 75[b] | 130 | 12 | 12 | 14 | 14 |
| $^{98}$Mo | 0.88[a] | 85 | 4.20[a] | 140 | | | 0.55 | 0.94 |
| $^{100}$Mo | 2.30[a] | 90 | 7.00[a] | 100 | | | 1.40 | 1.60 |
| $^{101}$Ru | 40[a] | 180 | 73[b] | 180 | 12 | 12 | 13 | 13 |
| $^{103}$Rh | 100[a] | 160 | 210[b] | 160 | 17 | 17 | 46 | 46 |
| $^{105}$Pd | 51[a] | 145 | 94[b] | 140 | 15 | 15 | 17 | 17 |
| $^{106}$Cd | 11[a] | 155 | 36[a] | 170 | | | 7.20 | 8.10 |
| $^{107}$Ag | 88 | 140 | 179[b] | 140 | 15 | 14 | 41 | 41 |
| $^{108}$Pd | 4.50[a] | 77 | 13[b] | 77 | | | 2.80 | 2.80 |
| $^{108}$Cd | 8.70[a] | 105 | 29[a] | 130 | | | 5.50 | 6.50 |
| $^{109}$Ag | 93 | 130 | 190[b] | 130 | 15 | 15 | 43 | 43 |
| $^{110}$Pd | 1.70[a] | 60 | 7.00[a] | 90 | | | 1.00 | 1.60 |
| $^{110}$Cd | 4.60[a] | 71 | 13[a] | 80 | | | 2.90 | 3.20 |
| $^{111}$Cd | 48[a] | 96 | 99[b] | 96 | 7.90 | 7.90 | 22 | 22 |
| $^{112}$Cd | 4.10[a] | 77 | 13[a] | 90 | | | 2.50 | 3.00 |
| $^{113}$Cd | 75[a] | 160 | 160[b] | 160 | 12 | 12 | 35 | 35 |
| $^{114}$Cd | 2.30[a] | 53 | 8.40[a] | 70 | | | 1.40 | 1.90 |
| $^{115}$In | 82[a] | 77 | 160[b] | 77 | 27 | 27 | 24 | 24 |
| $^{116}$Cd | 1.20[a] | 47 | 5.00[a] | 70 | | | 0.76 | 1.10 |
| $^{117}$Sn | 5.40[a] | 80 | 11[b] | 80 | 0.89 | 0.89 | 2.50 | 2.50 |
| $^{134}$Ba | 2.50[a] | 120 | 7.00[b] | 120 | | | 1.60 | 1.60 |
| $^{135}$Ba | 38[a] | 150 | 69[b] | 150 | 9.50 | 9.50 | 14 | 14 |

$$T_{\gamma J\pi}=2\pi S_{\gamma l}\frac{\rho_J}{\sum\rho_{J'}}\ , \tag{D15}$$

which is identical with (6.4). In some cases (e.g., $^{115}$In or $^{181}$Ta) the tabulated values of the strength functions are inconsistent with those of the widths (i.e., $S_{\gamma l}D_l=\langle\Gamma_{\gamma l}\rangle\sim\langle\Gamma_{\gamma 0}\rangle$ is not fulfilled); we then rejected the tabulated values for the strength functions and relied on the values for the widths.

We complete the extraction of input data with that of the neutron transmission coefficients, starting from the measured strength functions [51,52]:

$$S_l=\frac{\langle g\Gamma_n^l\rangle^{\rm red}}{(2l+1)D_l}\ . \tag{D16}$$

Here, the so-called reduced widths enter. They are related to the measured widths by

$$(\Gamma_n^l)^{\rm red}=\Gamma_{nl}^{\rm meas}(\sqrt{\epsilon}V_l)^{-1}\ , \tag{D17}$$

TABLE III. (*Continued*).

| Nucleus | $S_{\gamma 0}$ ($10^{-4}$) | $\Gamma_{\gamma 0}$ (meV) | $S_{\gamma 1}$ ($10^{-4}$) | $\Gamma_{\gamma 0}$ (meV) | $T_{\gamma,J_<,+}$ | $T_{\gamma,J_<,-}$ | $T_{\gamma,J_>,+}$ | $T_{\gamma,J_>,-}$ |
|---|---|---|---|---|---|---|---|---|
| | | | | | ($10^{-3}$) | | | |
| $^{137}$Ba | 2.80[a] | 80 | 5.10[b] | 80 | 0.70 | 0.70 | 1.00 | 1.00 |
| $^{139}$La | 2.60 | 54 | 3.60[a] | 40 | 0.81 | 0.60 | 0.82 | 0.61 |
| $^{140}$Ce | 0.11[a] | 35 | 0.27[a] | 30 | | | 0.07 | 0.06 |
| $^{143}$Nd | 18[a] | 80 | 33[b] | 80 | 5.50 | 5.50 | 5.60 | 5.60 |
| $^{144}$Nd | 1.30[a] | 54 | 3.60[b] | 54 | | | 0.79 | 0.79 |
| $^{145}$Nd | 34[a] | 75 | 64[b] | 75 | 11 | 11 | 11 | 11 |
| $^{146}$Nd | 2.30[a] | 54 | 2.80[a] | 23 | | | 1.40 | 0.61 |
| $^{148}$Nd | 3.60[a] | 51 | 10[b] | 51 | | | 2.30 | 2.30 |
| $^{149}$Sm | 282 | 62 | 530[b] | 62 | 88 | 88 | 90 | 90 |
| $^{150}$Sm | 11 | 60 | 19 | 37 | | | 6.90 | 4.20 |
| $^{150}$Nd | 3.90[a] | 67 | 11[b] | 67 | | | 2.40 | 2.40 |
| $^{152}$Sm | 12 | 62 | 8.00 | 15 | | | 7.50 | 1.80 |
| $^{153}$Eu | 719[a] | 93 | 1300[b] | 93 | 210 | 210 | 240 | 240 |
| $^{154}$Sm | 6.90 | 79 | 20[b] | 79 | | | 4.30 | 4.30 |
| $^{156}$Gd | 23 | 88 | 66[b] | 88 | | | 15 | 15 |
| $^{159}$Tb | 250 | 97 | 460[b] | 97 | 63 | 63 | 94 | 94 |
| $^{162}$Dy | 17 | 110 | 49[b] | 110 | | | 11 | 11 |
| $^{164}$Dy | 7.80 | 110 | 22[b] | 110 | | | 4.90 | 4.90 |
| $^{165}$Ho | 167 | 77 | 320[b] | 77 | 52 | 52 | 53 | 54 |
| $^{166}$Er | 24 | 92 | 69[b] | 92 | | | 15 | 15 |
| $^{169}$Tm | 140 | 100 | 300[b] | 100 | 23 | 23 | 65 | 66 |
| $^{170}$Er | 8.10 | 100 | 23[b] | 100 | | | 5.10 | 5.10 |
| $^{178}$Hf | 8.70 | 54 | 25[b] | 54 | | | 5.50 | 5.50 |
| $^{179}$Hf | 150 | 66 | 290[b] | 66 | 48 | 48 | 46 | 46 |
| $^{180}$Hf | 3.30 | 50 | 15[b] | 50 | | | 2.10 | 3.30 |
| $^{181}$Ta | 136 | 57 | 260[b] | 57 | 42 | 42 | 44 | 44 |
| $^{182}$W | 8.20 | 54 | 23[b] | 54 | | | 5.20 | 5.10 |
| $^{183}$W | 58 | 70 | 120[b] | 70 | 9.50 | 9.50 | 27 | 27 |
| $^{184}$W | 6.00 | 57 | 20[b] | 57 | | | 3.80 | 4.40 |
| $^{185}$Re | 179 | 56 | 340[b] | 56 | 51 | 52 | 62 | 62 |
| $^{186}$W | 5.80 | 50 | 16[b] | 50 | | | 3.60 | 3.60 |
| $^{186}$Os | 26 | 70 | 77[b] | 70 | | | 17 | 17 |
| $^{187}$Re | 139 | 57 | 260[b] | 57 | 40 | 40 | 48 | 48 |
| $^{187}$Os | 176 | 77 | 370[b] | 77 | 29 | 29 | 82 | 81 |
| $^{188}$Os | 20 | 83 | 59[b] | 83 | | | 13 | 13 |
| $^{197}$Au | 78 | 130 | 140[b] | 130 | 20 | 19 | 30 | 29 |
| $^{203}$Tl | 19 | 690 | 41[b] | 690 | 3.10 | 3.10 | 8.80 | 8.90 |
| $^{204}$Pb | 5.10[a] | 770 | 6.20[a] | 330 | | | 3.20 | 1.40 |
| $^{205}$Tl | 2.70 | 1500 | 5.70[b] | 1500 | 0.44 | 0.44 | 1.30 | 1.30 |
| $^{209}$Bi | 0.16 | 70 | 0.31 | 34 | 0.05 | 0.05 | 0.05 | 0.05 |
| $^{232}$Th | 14 | 24 | 41[b] | 24 | | | 8.90 | 9.00 |
| $^{235}$U | 795 | 35 | 1500[b] | 35 | 240 | 240 | 260 | 260 |
| $^{236}$U | 15 | 23 | 44[b] | 23 | | | 9.90 | 9.80 |
| $^{238}$U | 11 | 23 | 32[b] | 23 | | | 7.00 | 7.00 |

where the $V_l$ are given for low-energy neutrons by

$$V_0=1, \quad V_1=(kR)^2\approx 10^{-6}\rho^2\epsilon\ , \tag{D18}$$

here $\epsilon$ and $\rho$ are as explained around Eq. (5.3).

For convenience, we will think of measured widths in the following considerations and drop the superscript "meas". The average widths can be understood as average *first* within a pure sequence of given $J$ (running index $\lambda$) and *then* over $J$:

TABLE IV. Neutron strength functions for $s$-wave ($S_{n0}$) and $p$-wave ($S_{n1}$) resonances as in Mughabghab *et al.* [49,50] and corresponding transmission coefficients at 1 eV [Eq. (D23)].

| Nucleus | $S_{n0}$ ($10^{-4}$) | $S_{n1}$ ($10^{-4}$) | $T_{n0}(1)$ ($10^{-4}$) | $T_{n1}(1)$ ($10^{-9}$) |
|---|---|---|---|---|
| $^{32}$S | 0.73 | 0.57 | 4.59 | 0.32 |
| $^{40}$Ca | 3.20 | 0.17 | 20.11 | 0.11 |
| $^{43}$Ca | 3.30 | 0.37 | 20.73 | 0.25 |
| $^{50}$Cr | 3.60 | 0.33 | 22.62 | 0.25 |
| $^{52}$Cr | 2.50 | 0.52 | 15.71 | 0.40 |
| $^{54}$Fe | 8.70 | 0.58 | 54.66 | 0.46 |
| $^{55}$Mn | 3.90 | 0.35 | 24.50 | 0.28 |
| $^{56}$Fe | 2.60 | 0.45 | 16.34 | 0.36 |
| $^{57}$Fe | 4.20 | 0.20 | 26.39 | 0.16 |
| $^{58}$Fe | 3.60 | 0.60 | 22.62 | 0.50 |
| $^{58}$Ni | 2.80 | 0.50 | 17.59 | 0.41 |
| $^{60}$Ni | 2.70 | 0.30 | 16.96 | 0.25 |
| $^{62}$Ni | 2.80 | 0.30 | 17.59 | 0.26 |
| $^{63}$Cu | 2.30 | 0.30 | 14.45 | 0.26 |
| $^{64}$Ni | 2.90 | 0.60 | 18.22 | 0.53 |
| $^{64}$Zn | 1.70 | 0.60 | 10.68 | 0.53 |
| $^{66}$Zn | 1.90 | 0.70 | 11.94 | 0.63 |
| $^{68}$Zn | 2.20 | 0.39 | 13.82 | 0.36 |
| $^{77}$Se | 1.28 | 0.76 | 8.04 | 0.76 |
| $^{78}$Se | 1.23 | 1.73 | 7.73 | 1.75 |
| $^{80}$Se | 1.61 | 0.50 | 10.12 | 0.51 |
| $^{85}$Rb | 1.00 | 3.30 | 6.28 | 3.53 |
| $^{88}$Sr | 0.45 | 4.98 | 2.83 | 5.45 |
| $^{89}$Y | 0.27 | 2.64 | 1.70 | 2.91 |
| $^{90}$Zr | 0.70 | 4.00 | 4.40 | 4.44 |
| $^{91}$Zr | 0.36 | 6.70 | 2.26 | 7.50 |
| $^{92}$Zr | 0.50 | 7.00 | 3.14 | 7.89 |
| $^{92}$Mo | 0.50 | 4.70 | 3.14 | 5.30 |
| $^{93}$Nb | 0.60 | 5.80 | 3.77 | 6.59 |
| $^{94}$Zr | 0.50 | 9.80 | 3.14 | 11.21 |
| $^{94}$Mo | 0.53 | 4.60 | 3.33 | 5.26 |
| $^{95}$Mo | 0.35 | 7.00 | 2.20 | 8.06 |
| $^{96}$Mo | 0.43 | 8.70 | 2.70 | 10.09 |
| $^{97}$Mo | 0.37 | 6.00 | 2.32 | 7.01 |
| $^{98}$Mo | 0.54 | 3.60 | 3.39 | 4.23 |
| $^{100}$Mo | 0.73 | 4.40 | 4.59 | 5.24 |
| $^{101}$Ru | 0.54 | 6.10 | 3.39 | 7.32 |
| $^{103}$Rh | 0.53 | 5.50 | 3.33 | 6.68 |
| $^{105}$Pd | 0.60 | 5.80 | 3.77 | 7.14 |
| $^{106}$Cd | 1.00 | 5.00 | 6.28 | 6.19 |
| $^{107}$Ag | 0.38 | 3.80 | 2.39 | 4.74 |
| $^{108}$Pd | 0.78 | 4.40 | 4.90 | 5.52 |
| $^{108}$Cd | 1.20 | 4.80 | 7.54 | 6.02 |
| $^{109}$Ag | 0.46 | 3.80 | 2.89 | 4.80 |
| $^{110}$Pd | 0.40 | 6.00 | 2.51 | 7.62 |
| $^{110}$Cd | 0.44 | 3.00 | 2.76 | 3.81 |
| $^{111}$Cd | 0.80 | 3.00 | 5.03 | 3.83 |
| $^{112}$Cd | 0.50 | 4.40 | 3.14 | 5.65 |
| $^{113}$Cd | 0.31 | 2.20 | 1.95 | 2.84 |
| $^{114}$Cd | 0.64 | 3.50 | 4.02 | 4.55 |
| $^{115}$In | 0.26 | 3.20 | 1.63 | 4.19 |
| $^{116}$Cd | 0.16 | 2.80 | 1.01 | 3.68 |
| $^{117}$Sn | 0.21 | 3.00 | 1.32 | 3.97 |
| $^{134}$Ba | 0.53 | 0.80 | 3.33 | 1.16 |
| $^{135}$Ba | 0.90 | 0.48 | 5.65 | 0.70 |
| $^{137}$Ba | 0.41 | 0.31 | 2.58 | 0.46 |
| $^{139}$La | 0.78 | 0.40 | 4.90 | 0.59 |
| $^{140}$Ce | 1.10 | 0.34 | 6.91 | 0.51 |
| $^{143}$Nd | 3.20 | 0.80 | 20.11 | 1.21 |
| $^{144}$Nd | 4.00 | 0.50 | 25.13 | 0.76 |
| $^{145}$Nd | 4.40 | 0.80 | 27.65 | 1.22 |
| $^{146}$Nd | 2.60 | 0.50 | 16.34 | 0.77 |
| $^{148}$Nd | 3.00 | 0.30 | 18.85 | 0.46 |
| $^{149}$Sm | 4.60 | 0.30 | 28.90 | 0.47 |
| $^{150}$Sm | 3.60 | 0.80 | 22.62 | 1.25 |
| $^{150}$Nd | 3.00 | 0.80 | 18.85 | 1.25 |
| $^{152}$Sm | 2.20 | 0.55 | 13.82 | 0.87 |
| $^{153}$Eu | 2.50 | 0.30 | 15.71 | 0.47 |
| $^{154}$Sm | 1.80 | 0.80 | 11.31 | 1.27 |
| $^{156}$Gd | 1.70 | 0.55 | 10.68 | 0.88 |
| $^{159}$Tb | 1.55 | 1.90 | 9.74 | 3.08 |
| $^{162}$Dy | 1.80 | 1.10 | 11.31 | 1.81 |
| $^{164}$Dy | 1.70 | 1.30 | 10.68 | 2.15 |
| $^{165}$Ho | 1.80 | 0.63 | 11.31 | 1.05 |
| $^{166}$Er | 1.60 | 0.94 | 10.05 | 1.57 |
| $^{169}$Tm | 1.60 | 1.01 | 10.05 | 1.71 |
| $^{170}$Er | 1.50 | 0.94 | 9.42 | 1.60 |
| $^{178}$Hf | 2.20 | 0.51 | 13.82 | 0.89 |
| $^{179}$Hf | 1.70 | 0.83 | 10.68 | 1.46 |
| $^{180}$Hf | 1.90 | 0.44 | 11.94 | 0.78 |
| $^{181}$Ta | 1.70 | 0.20 | 10.68 | 0.35 |
| $^{182}$W | 2.20 | 0.72 | 13.82 | 1.28 |
| $^{183}$W | 1.70 | 0.72 | 10.68 | 1.28 |
| $^{184}$W | 2.50 | 0.58 | 15.71 | 1.04 |
| $^{185}$Re | 2.10 | 1.70 | 13.19 | 3.05 |
| $^{186}$W | 2.10 | 0.37 | 13.19 | 0.67 |
| $^{186}$Os | 2.20 | 0.25 | 13.82 | 0.45 |
| $^{187}$Re | 2.50 | 1.00 | 15.71 | 1.81 |
| $^{187}$Os | 3.10 | 0.35 | 19.48 | 0.63 |
| $^{188}$Os | 2.30 | 0.30 | 14.45 | 0.54 |
| $^{197}$Au | 2.00 | 0.40 | 12.57 | 0.75 |
| $^{203}$Tl | 1.60 | 0.29 | 10.05 | 0.55 |
| $^{204}$Pb | 0.65 | 0.23 | 4.08 | 0.44 |
| $^{205}$Tl | 0.78 | 0.17 | 4.90 | 0.33 |
| $^{209}$Bi | 0.65 | 0.25 | 4.08 | 0.49 |
| $^{232}$Th | 0.84 | 1.48 | 5.28 | 3.09 |
| $^{235}$U | 1.00 | 1.80 | 6.28 | 3.79 |
| $^{236}$U | 1.00 | 2.30 | 6.28 | 4.86 |
| $^{238}$U | 1.20 | 1.70 | 7.54 | 3.61 |

$$\langle g\Gamma_n^l\rangle=\left\langle\frac{2J+1}{2(2I+1)}\Gamma_{n,l,J,\lambda}\right\rangle_{J,\lambda}$$
$$=\left\langle\frac{2J+1}{2(2I+1)}\bar{\Gamma}^{\lambda}_{n,l,J,\lambda}\right\rangle_{J}$$
$$=\sum_J \omega_J\frac{2J+1}{2(2I+1)}\bar{\Gamma}_{n,l,J}\ . \tag{D19}$$

Here, we have denoted the averages over $\lambda$ with a bar together with the index; then we have rewritten the average over $J$ as a weighted sum, as in the preceding considerations. The width for given $J$ is, in turn, a sum over partial widths for all allowed values of $j$

$$\Gamma_{n,l,J}=\sum_{j=l\pm1/2}\Delta(j,I,J)\Gamma_{n,l,j,J}\ , \tag{D20}$$

where $\Delta(j,I,J)$ is unity for the triangle rule $|I-j|\le j\le I+j$ fulfilled and zero otherwise. Note that we think of widths as being *measured*, not reduced ones (as in Mughabghab *et al.* [51,52]). Using subsequently (D20), the definition of the $\omega_J$, Eq. (D11), the relationships (D3) and (D4), and the definition of the $T_c$, Eq. (6.1), we obtain

$$\langle g\Gamma_n^l\rangle=\sum_{J=|I-l-1/2|}^{I+l+1/2}\frac{\rho_J}{\sum\rho_{J'}}\frac{2J+1}{2(2I+1)}\sum_{j=l\pm1/2}\Delta(j,I,J)\bar{\Gamma}_{n,l,j,J}$$
$$=D_l\sum_{J=|I-l-1/2|}^{I+l+1/2}\frac{2J+1}{2(2I+1)}\sum_{j=l\pm1/2}\Delta(j,I,J)\frac{\bar{\Gamma}_{n,l,j,J}}{d^{J\pi}}$$
$$=\frac{1}{2\pi}D_l\sum_{J=|I-l-1/2|}^{I+l+1/2}\frac{2J+1}{2(2I+1)}\sum_{j=l\pm1/2}\Delta(j,I,J)T_{n,l,j,J}\ . \tag{D21}$$

We now assume that the neutron transmission coefficients are independent of $J$ as well as of $j$. This latter assumption certainly can be improved by using optical model codes including a spin-orbit term. In some cases, this may lead to corrections up to 20–30 %. Solving for the transmission coefficient, our simplification leads to

$$T_{n,l,j,J}=2\pi\left[\sum_{j,J}\Delta(j,I,J)\frac{2J+1}{2(2I+1)}\right]^{-1}\frac{\langle g\Gamma_n^l\rangle}{D_l}\ . \tag{D22}$$

If we introduce the reduced widths of Eqs. (D16) and (D17), we have established the desired result between neutron-transmission coefficients and strength functions

$$T_{n,l,j,J}\overset{\text{def}}{=}T_{n,l}$$
$$=2\pi(2l+1)\left[\sum_{j,J}\Delta(j,I,J)\frac{2J+1}{2(2I+1)}\right]^{-1}\frac{\langle g\Gamma_n^l\rangle}{(2l+1)D_l}\sqrt{\epsilon}V_l$$
$$=2\pi(2l+1)\left[\sum_{j,J}\Delta(j,I,J)\frac{2J+1}{2(2I+1)}\right]^{-1}\sqrt{\epsilon}V_lS_l\ . \tag{D23}$$

(The summation limits are $j=l\pm\frac{1}{2}$, $|I-l-\frac{1}{2}|\le J\le I+l+\frac{1}{2}$.) This result can be interpreted in the following way: up to the conventional weight factor $2\pi(2l+1)2(2I+1)/(2J+1)$, the sum in (D23) just counts the number of open channels which can be fed by a $l$ wave; if all of these channels show equal transmission, dividing by their number means distributing the strength $S_l$ equally among all of them. Specializing (D23) to the cases $l=0$ and $l=1$ and evaluating the normalizing sum we obtain (5.2).

We conclude this appendix with a survey of the data we have used and extracted. Table II shows the level densities, Table III the sum of $\gamma$-transmission coefficients and Table IV the neutron transmission coefficients.

[1] Y. G. Abov, P. A. Krupchitsky, and Y. A. Oratovsky, Phys. Lett. **12**, 25 (1964).
[2] T. E. O. Ericson, Phys. Lett. **23**, 97 (1966).
[3] I. S. Shapiro, Usp. Fiz. Nauk. **95**, 647 (1968) [Sov. Phys. Usp. **11**, 582 (1969)].
[4] P. A. Krupchitsky, *Fundamental Research with Polarized Slow Neutrons* (Springer, Berlin, 1987).
[5] V. P. Alfimenkov *et al.*, Pis'ma Zh. Eksp. Teor. Fiz. **35**, 42 (1982) [JETP Lett. **35**, 51 (1982)].
[6] O. P. Sushkov and V. V. Flambaum, Pis'ma Zh. Eksp. Teor. Fiz. **32**, 377 (1980) [JETP Lett. **32**, 352 (1980)].
[7] C. D. Bowman, J. D. Bowman, and V. W. Yuan, Phys. Rev. C **39**, 1721 (1989).
[8] V. E. Bunakov and V. P. Gudkov, Z. Phys. A **303**, 285 (1981).
[9] O. P. Sushkov and V. V. Flambaum [Sov. Phys. Usp **25**, 1 (1982)].
[10] V. E. Bunakov and V. P. Gudkov, Nucl. Phys. **A401**, 93 (1983).
[11] J. J. M. Verbaarschot, H. A. Weidenmüller, and M. R. Zirnbauer, Phys. Rep. **129**, 367 (1985).
[12] J. D. Bowman *et al.*, Phys. Rev. Lett. **65**, 1192 (1990).
[13] V. E. Bunakov and V. P. Gudkov, Z. Phys. A **308**, 363 (1982).
[14] D. Boosé, H. L. Harney, and H. A. Weidenmüller, Phys. Rev. Lett. **56**, 2012 (1986).
[15] D. Boosé, H. L. Harney, and H. A. Weidenmüller, Z. Phys. A **325**, 363 (1986).
[16] E. D. Davis, in *Fundamental Symmetries and Nuclear Structure,* Proceedings of the Workshop, Santa Fe, 1988, edited by J. N. Ginocchio and S. P. Rosen (World Scientific, Singapore, 1989).
[17] E. D. Davis, Phys. Lett. B **226**, 197 (1989).
[18] C. D. Bowman *et al.*, in *Fundamental Symmetries and Nuclear Structure* [16].
[19] C. R. Gould *et al.*, Int. J. Mod. Phys. A **5**, 2181 (1990).
[20] L. Stodolsky, Phys. Lett. **50B**, 353 (1974).
[21] G. E. Bacon, *Neutron Diffraction* (Clarendon, Oxford, 1962).
[22] M. Simonius, in *Proceedings of the 6th International Symposium on Polarization Phenomena in Nuclear Physics,* edited by M. Kondo *et al.* [J. Phys. Soc. Jpn. Suppl. **55**, 523 (1986)].
[23] S. Kistryn *et al.*, Phys. Rev. Lett. **58**, 1616 (1987).
[24] P. D. Eversheim *et al.*, Phys. Lett. B **256**, 11 (1991).
[25] *Mathematisches Wörterbuch,* edited by J. Naas and H. L. Schmid (Teubner Verlag, Stuttgart, 1962).
[26] Y. Yamaguchi, J. Phys. Soc. Jpn. **57**, 1518 (1988).
[27] C. Mahaux and H. A. Weidenmüller, *Shell Model Approach to Nuclear Reactions* (North Holland, Amsterdam, 1969).
[28] J. J. M. Verbaarschot, Ann. Phys. (N.Y.) **168**, 368 (1986).
[29] H. Nishioka and H. A. Weidenmüller, Phys. Lett. **157B**, 101 (1985).
[30] H. Nishioka, J. J. M. Verbaarschot and H. A. Weidenmüller, Ann. Phys. (N.Y.) **172**, 67 (1986).
[31] H. L. Harney, A. Richter, and H. A. Weidenmüller, Rev. Mod. Phys. **58**, 607 (1987).
[32] H. L. Harney and A. Hüpper, Z. Phys. A **328**, 327 (1987).
[33] H. L. Harney, A. Hüpper, M. Mayer, and A. Müller, Z. Phys. A **335**, 293 (1990).
[34] A. Müller and H. L. Harney, Z. Phys. A **337**, 465 (1990).
[35] H. L. Harney (unpublished results).
[36] M. Abramowitz and I. A. Stegun, *Pocketbook of Mathematical Functions* (Harri Deutsch, Thun, 1984).
[37] A. Müller and H. L. Harney, Phys. Rev. C **35**, 1228 (1987).
[38] E. Akkermans and R. Maynard, J. Phys. Lett. (Paris) **46**, L-1045 (1985).
[39] J. B. French, A. Pandey, and J. Smith, in *Tests of Time Reversal Invariance in Neutron Physics,* Proceedings of the Workshop, Chapel Hill, 1987, edited by N. R. Roberson, C. R. Gould, and J. D. Bowman (World Scientific, Singapore, 1987), p. 80.
[40] V. E. Bunakov, Phys. Rev. Lett. **60**, 2250 (1988).
[41] M. B. Johnson, J. D. Bowman, and S. H. Yoo, Phys. Rev. Lett. **67**, 310 (1991).
[42] D. F. Zaretskij and V. K. Sirotkin, Yad. Fiz. **42**, 885 (1985) [Sov. J. Nucl. Phys. **42**, 561 (1985)].
[43] R. J. Blin-Stoyle, Phys. Rev. **120**, 181 (1960).
[44] F. T. Smith, Phys. Rev. **118**, 349 (1960).
[45] T.-Y. Wu and T. Ohmura, *Quantum Theory of Scattering* (Prentice Hall, Englewood Cliffs, NJ, 1962), Sec. W5.
[46] J. M. Blatt and V. F. Weisskopf, *Theoretical Nuclear Physics* (Springer, Berlin, 1979).
[47] D. Boosé, H. L. Harney, and H. A. Weidenmüller, Phys. Rev. Lett. **56**, 2012 (1986).
[48] M. Quack, Angew. Chem. **101**, 588 (1989).
[49] V. L. Lyuboshits, Yad. Fiz. **27**, 948 (1978) [Sov. J. Nucl. Phys. **27**, 502 (1978)].
[50] V. L. Lyuboshits, Phys. Lett. **72B**, 41 (1977).
[51] S. F. Mughabghab, M. Divadeenam, and N. E. Holden, *Neutron Cross Sections* (Academic, New York, 1981), Vol. 1A.
[52] S. F. Mughabghab, *Neutron Cross Sections* (Academic, New York, 1984), Vol. 1B.
[53] H. Vonach and M. Hille, Nucl. Phys. **A127**, 289 (1969).
[54] W. Dilg *et al.*, Nucl. Phys. **A217**, 269 (1973).
[55] T. von Egidy, H. H. Schmidt, and A. N. Behkami, Nucl. Phys. **A481**, 189 (1988).
[56] *Handbook of Chemistry and Physics,* edited by R. C. Weast (CRC, Boca Raton, 1988), p. B-5.
[57] V. E. Bunakov, private communication.
[58] V. E. Bunakov, E. D. Davis, and H. A. Weidenmüller, Phys. Rev. C **42**, 1718 (1990).
[59] E. D. Davis, Z. Phys. A **340**, 159 (1991).
[60] H. A. Weidenmüller, Nucl. Phys. **A522**, 293c (1991).
[61] V. E. Bunakov and A. Müller, in preparation.
[62] C. M. Franle *et al.*, Phys. Rev. Lett. **67**, 564 (1991).
[63] H. A. Weidenmüller, private communication.
[64] I. N. Bronstein and K. A. Semendjajew, *Taschenbuch der Mathematik* (Harri Deutsch, Thun, 1980).